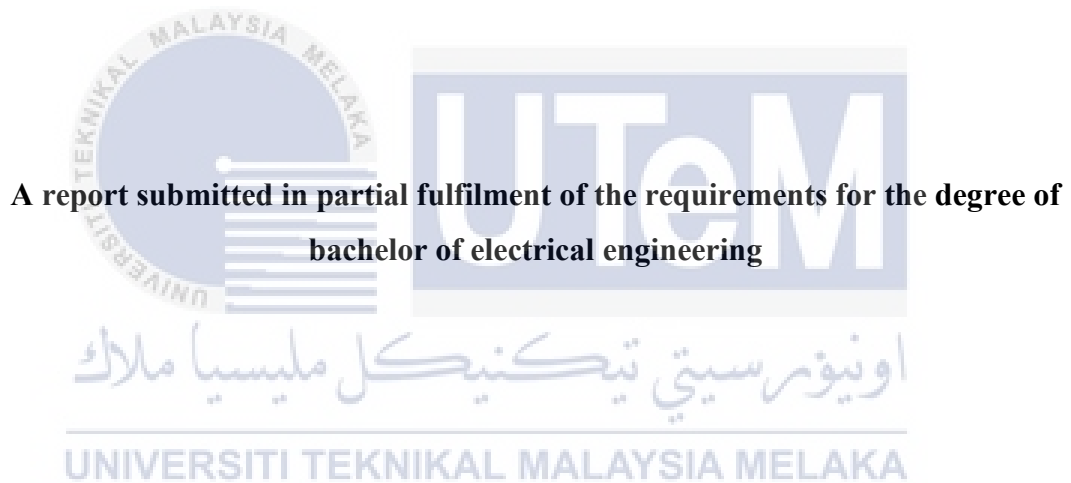


**REDUCED TORQUE RIPPLE OF DIRECT TORQUE CONTROL OF  
INDUCTION MOTOR USING HYSTERESIS BASED CONTROLLER**

**ASHRAF NUKMAN BIN AZLAN**



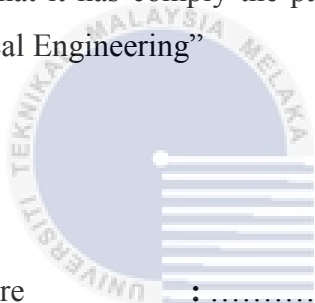
**A report submitted in partial fulfilment of the requirements for the degree of  
bachelor of electrical engineering**

**Faculty of Electrical Engineering**

**UNIVERSITI TEKNIKAL MALAYSIA MELAKA**

**2018**

“I hereby declare that I have read through this report entitle “*Reduced Torque Ripple of Direct Torque Control of Induction Motor Using Hysteresis Based Controller*” and found that it has comply the partial fulfilment for awarding the degree of Bachelor of Electrical Engineering”



Signature : .....

اونيورسيتي تیکنیکل ملیسیا ملاک

Supervisor's Name : Dr. Auzani Bin Jidin

Date : JUNE 2018

I declare that this report entitles “*Reduced Torque Ripple of Direct Torque Control of Induction Motor Using Hysteresis Based Controller*” is the result of my own research except as cited in the reference. The report has not been accepted for any degree and is not concurrently submitted in candidate of any other degree.

**Signature**

: .....

**Name**

: Ashraf Nukman Bin Azlan

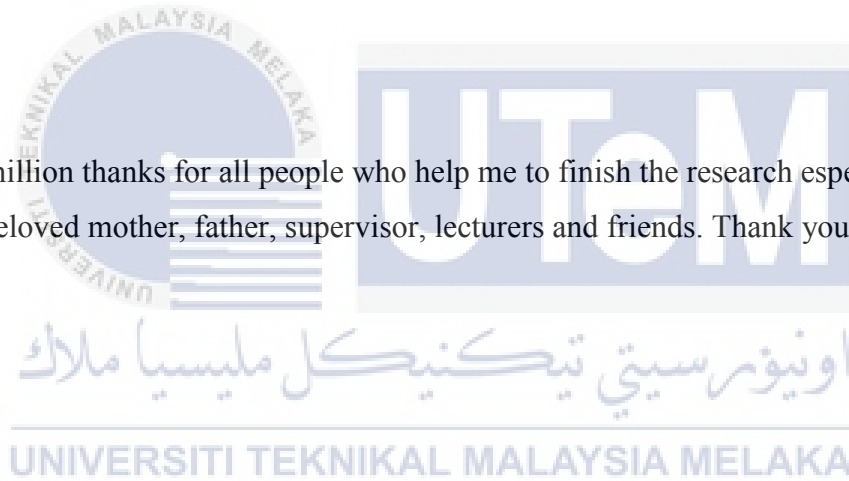
UNIVERSITI TEKNIKAL MALAYSIA MELAKA

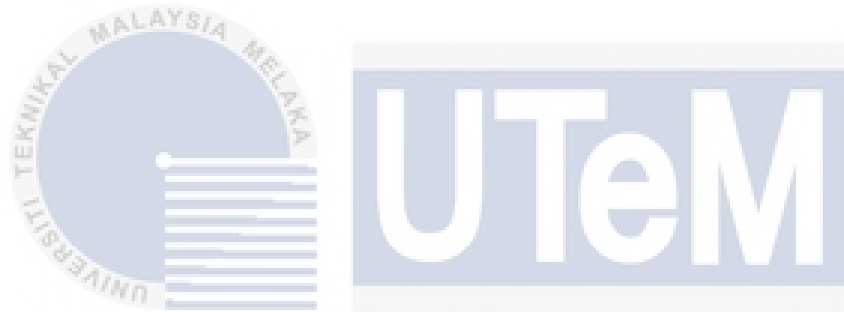
**Date**

: JUNE 2018

## DEDICATION

A million thanks for all people who help me to finish the research especially to my beloved mother, father, supervisor, lecturers and friends. Thank you everyone.





اونيورسيتي تيكنيكل مليسيا ملاك

UNIVERSITI TEKNIKAL MALAYSIA MELAKA



## **FACULTY OF ELECTRICAL ENGINEERING**



### **REDUCED TORQUE RIPPLE OF DIRECT TORQUE CONTROL OF INDUCTION MOTOR USING HYSTERESIS BASED CONTROLLER**

**NAME : ASHRAF NUKMAN BIN AZLAN**  
**NO. MATRIX : B011510013**  
**SUPERVISOR : Dr. AUZANI BIN JIDIN**  
**PANEL : Prof. Madya Dr. KASRUL BIN KARIM**

## ACKNOWLEDGEMENT

In preparing this report, I was contact with many people, researchers, academicians and technicians. They have contributed towards my understanding and thought. In particular, I wish to express my sincere appreciation to my main project supervisor, Dr. Auzani Bin Jidin, for encouragement guidance, critics and friendship. I am also very thankful to Miss Siti Azura Binti Ahmad Tarusan for her guidance, advices and motivation.

My fellow undergraduate students should also be recognised for their support. My sincere appreciation also extends to all my colleagues and others who have provided assistance at various occasions. Their views and tips are useful indeed. Unfortunately, it is not possible to list all of them in this limited space. Last but not least, I am grateful to all my family members for their endless support.

UNIVERSITI TEKNIKAL MALAYSIA MELAKA

## ABSTRACT

Alternating Current (AC) motor drives required the precision and faster response controller to achieve the excellent and optimal performance. Therefore, the vector control has been introduced to control the AC drive, either steady-state or dynamic response. One of the vector control method is Field Oriented Control (FOC) to control the AC motor. Although the FOC is the first controlling method was introduced, but this vector control method is complicated configuration and difficult to design. After a few decades, Direct Torque Control (DTC) was introduced. This vector control scheme is popular method, simplest structure and easy implementation for controlling the AC motor. DTC is widely used in industry as well as the electric vehicles because it is easy to design the configuration. Asynchronous motor is one of the AC motor. Asynchronous motor namely induction motor has some advantages due to economical, maintenance and weight. The conventional DTC controller has some major problems such as high torque ripple and switching devices do not operate at optimal performance during hardware implementation. The switching frequency controlled by the Voltage Source Inverter (VSI). DTC drive can operate at different of speed condition with applied the voltage vector which generated by using Voltage Source Inverter (VSI) by appropriate selection of voltage vectors. To improve the performance of induction motor, this thesis proposed a new topology circuit of VSI to ensure the switching devices operate at optimal performance. The torque is controlled by using hysteresis-based controller. The tolerant band of the hysteresis band are being control as the performances of the motor will improve. In summary, the torque is reduced by the hysteresis-based controller and the switching frequency is being adapted by new structure of switching devices.

## ABSTRAK

Pemacu motor Arus Ulang-alik (AC) memerlukan pengawal tindak balas yang lebih pantas dan pantas untuk mencapai prestasi cemerlang dan optimum. Oleh itu, kawalan vektor telah diperkenalkan untuk mengawal pemacu AC, sama ada tindak balas mantap atau dinamik. Salah satu kaedah kawalan vektor adalah Kawalan Berorientasikan Lapangan (FOC) untuk mengawal motor AC. Walaupun FOC adalah kaedah kawalan pertama diperkenalkan, tetapi kaedah kawalan vektor ini adalah konfigurasi rumit dan sukar untuk direkabentuk. Selepas beberapa dekad, Kawalan Langsung Tork (DTC) diperkenalkan. Skim kawalan vektor ini adalah kaedah yang popular, struktur mudah dan pelaksanaan yang mudah untuk mengawal motor AC. DTC digunakan secara meluas dalam industri serta kenderaan elektrik kerana mudah untuk merancang konfigurasi. Motor tidak sejajar adalah salah satu motor AC. Motor tidak sejajar iaitu motor induksi mempunyai beberapa kelebihan terhadap ekonomi, penyelenggaraan dan berat. Pengawal DTC konvensional mempunyai beberapa masalah utama seperti riak tork tinggi dan peranti pensuisan tidak beroperasi pada prestasi optimum semasa pelaksanaan perkakasan. Kekerapan menukar yang dikawal oleh Sumber Voltan Penyongsang (VSI). Pemacu DTC boleh beroperasi pada keadaan kelajuan yang berbeza dengan menggunakan vektor voltan yang dihasilkan dengan menggunakan Sumber Voltan Penyongsang (VSI) dengan pemilihan vektor voltan yang sesuai. Untuk meningkatkan prestasi motor induksi, tesis ini mencadangkan litar topologi baru VSI untuk memastikan peranti pensuisan beroperasi pada prestasi optimum. Tork dikawal dengan menggunakan pengawal berasaskan histerisis. Toleran pengikat histeris dikecilkan menyebabkan prestasi motor akan bertambah baik. Ringkasnya, tork dikurangkan oleh pengawal berasaskan histeresis dan kekerapan penukaran disesuaikan dengan struktur peranti pensuisan baru.

## TABLE OF CONTENT

CHAPTER	TITLE	PAGE
	ACKNOWLEDGEMENT	i
	ABSTRACT	ii
	ABSTRAK	iii
	TABLE OF CONTENTS	iv
	LIST OF TABLES	vi
	LIST OF FIGURES	vii
	LIST OF APPENDICES	ix
1	INTRODUCTION	
	1.1 Research Background and Motivation	1
	1.2 Problem Statement	5
	1.3 Research Objective	6
	1.4 Project Scope	6
	1.5 Report Outline	7
2	LITERATURE REVIEW	
	2.1 Introduction	8
	2.2 Asynchronous Motor	9
	2.3 Operating Principle	9
	2.4 Voltage Source Inverter (VSI)	10
	2.5 Control Strategy of Induction Motor	10
	2.5.1 Direct Torque Control	11
	2.6 Performance Improvements of Direct Torque Control	13
3	RESEARCH METHODOLOGY	
	3.1 Introduction	14

3.2	Mathematical Modelling of Three Phase Induction Motor	15
3.3	Three Phase Voltage Source Inverter (VSI)	19
3.3.1	Topology Circuit of VSI	19
3.3.2	Mapping of Voltage Vector	20
3.3.3	Clarke Transformation	21
3.4	Estimation of Torque and Flux	24
3.5	Principle Control of Torque and Flux	25
3.5.1	Hysteresis Controller	26
3.5.2	Control of Torque	27
3.5.3	Control of Stator Flux	31
3.6	Sector Detection	34
3.7	Complete Circuit of Direct Torque Control of Induction Motor	35
3.8	Proposed Technique	38
3.9	Hardware Implementation	40
3.9.1	Blanking Time	41
3.10	Flowchart	42
4	RESULT AND DISCUSSION	
4.1	Introduction	45
4.2	Conventional Result	45
4.3	Proposed Technique Simulation Result	49
4.4	Hardware Result	56
5	CONCLUSION AND RECOMMENDATION	
5.1	Conclusion	59
5.2	Recommendation	60
	REFERENCES	61
	APPENDICES	63

**LIST OF TABLES**

<b>TABLE</b>	<b>TITLE</b>	<b>PAGE</b>
3.1	Look-up Table	34



## LIST OF FIGURES

FIGURE	TITLE	PAGE
1.1	Structure of FOC of Induction Motor	2
1.2	Structure of DTC of Induction Motor	3
1.3	Structure of DSC of Induction Motor	4
2.1	Topology Circuit of Voltage Source Inverter	10
2.2	Overview of Torque and Flux Controller	12
2.3	General Structure of Direct Torque Control	12
3.1	Cross Section of Single Pole Three Phase Motor	16
3.2	Topology Circuit of Voltage Source Inverter	19
3.3	Simplified Voltage Source Inverter Circuit	20
3.4	Voltage Vector with Switching Status in VSI	21
3.5	Three phase sinusoidal waveform	21
3.6	Voltage Vector of Three Phase	22
3.7	Two Phase Voltage	23
3.8	Operation of Hysteresis Controller	26
3.9	Stator and Rotor Flux Vector	28
3.10	Active Forward Voltage Vector	28
3.11	Zero Voltage Vector	29
3.12	Active Reverse Voltage Vector	29
3.13	Three Level Hysteresis Controller	30
3.14	Waveform of Torque, Torque Error & Torque Error Status	30
3.15	Trajectory of Stator Flux	32
3.16	Two Level Hysteresis Controller	33
3.17	Waveform of Stator Flux, Flux Error & Flux Error Status	33
3.18	Complete Simulation Circuit of DTC	36
3.19	Mathematical Modelling for Voltage Components	36
3.20	Mathematical Modelling for Current Components	37
3.21	Expression of Estimation Torque, Estimation Flux and Angle	37
3.22	Proposed Technique	39

3.23	Group of Four Switching Devices	39
3.24	Structure of Voltage Source Inverter	40
3.25	Dspace Connector	41
3.26	Microcontroller FPGA	42
3.27	Block Diagram of Blanking Time Generation	42
3.28	Flowchart of Research Methodology	43
4.1	DTC operation Circuit	46
4.2	Estimation Torque, Torque, Torque Error & Torque Error Status	47
4.3	Comparison of Waveforms	48
4.4	VSI Connection	48
4.5	Switching Frequency of VSI	49
4.6	Configuration of DTC	50
4.7	Reference Torque, Torque, Torque Error & Torque Error Status	51
4.8	Comparison of Waveforms	52
4.9	1 <sup>st</sup> Leg Switching Frequency of VSI	53
4.10	Proposed Strategy	53
4.11	Pulses	54
4.12	Switching Devices Operate Alternately	55
4.13	Phases Current	56
4.14	Proposed Switching Technique	57
4.15	Proposed Switching Technique	57
4.16	Dead Time	58
4.17	Phases Current	58

**LIST OF APPENDICES**

<b>APPENDIX</b>	<b>TITLE</b>	<b>PAGE</b>
A	Machine Parameter	63
B	Sector Selection Function	64
C	Gantt Chart	65





اونيورسيتي تيكنيكل مليسيا ملاك

UNIVERSITI TEKNIKAL MALAYSIA MELAKA

## CHAPTER 1

### INTRODUCTION

#### 1.1 Research Background and Motivation

Several decades ago, almost all industries used brush Direct Current (DC) motor drive due to its structure and fast torque dynamic control. The fast dynamic control can be run by controlling the armature current due to the armature current is always perpendicular to the magnetic flux. However, the brush DC motor is expensive, high maintenance and not able to operate at very high speeds. The construction of brush DC motor based on commutator and brushes which can contribute limitation such as frictional. In addition, the brush DC motor requires regular maintenance due to degrading of winding insulator, particularly for the dc motor applications that require at high speed and high current or dirty environment. Due to the mentioned limitation, nowadays, there is a type of Alternative Current (AC) motor known to offer less maintenance requires, rugged and high efficiency. This AC motor is preferable for many industrial applications. Since 1970's, several vector control technique were introduced to provide excellent dynamic control performance compare to DC motor drives. [1]

At early stage, the vector control called as Field Oriented Control (FOC) was introduced in 1972 by Blaschke which enables to control the torque and flux using their respective current producing components in synchronous reference frame. In such way, the current components are DC quantities, so the armature current and field

current in DC motor drive which control the torque and flux respectively. However, FOC needs a frame of transformer to convert the DC quantities of the currents to phase current. In addition, the FOC method required knowledge of machine parameters, speed information and current controllers to establish the control of torque and flux. In other words, FOC is a method with complex structure of design. Figure 1.1 shown the whole structure of Field Oriented Control (FOC).

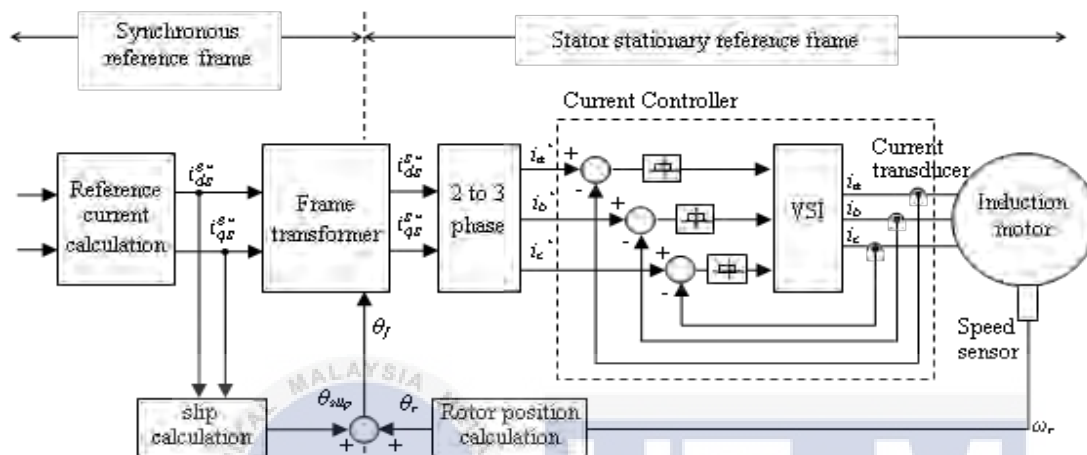


Figure 1.1: Structure of FOC of Induction Machine

After a few years later, a new method to control the torque and flux was introduced by Takahashi and Noguchi called Direct Torque Control (DTC). The structure of DTC is simpler than the structure of FOC. Figure 1.2 shows the DTC general structure which eliminates the use of current controller, frame of transformer and the speed sensor. In addition, the DTC method has less sensitivity on parameter variations due to the changes of temperature. Since, the DTC does not totally depends on machine parameters to estimate the control parameters, as the FOC control method. DTC is the simplest method model to estimate the stator flux which only required a stator resistance information. A decouple control structure employed in DTC scheme, where the torque is being controlled by using three-level hysteresis comparator while the flux is controlled by using two-level hysteresis comparator as shown in Figure 1.2. The comparators are used to restrict the errors within the limitation of the hysteresis bands by providing error statuses to the switching table. So, the restriction errors can be accomplished as the switching states to switch the appropriate voltage vector. The

appropriate selection of voltage vector, can control the torque and flux. Figure 1.2 below shows the structures of Direct Torque Control (DTC).

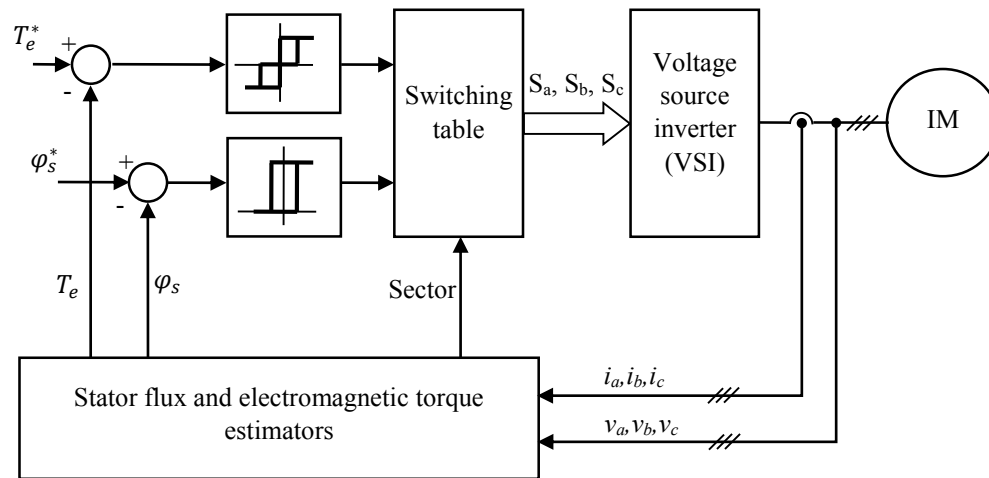


Figure 1.2: Structure of DTC of Induction Machine

In 1985, Depenbrock proposed a new method to control the induction motor call Direct Self Control (DSC). The Direct Self Control (DSC) method makes the induction motor possible to achieve precise control of torque and speed in an inverter-fed induction motor drive system. The DSC is well suited to high power drives with low switching frequency. The DSC method gives an inverter and fed into induction motor with excellent dynamic performance. The DSC control method is the improvement from DTC method but the DSC general structure is more complex compared to DTC. The control principle of the torque and flux are same with the DTC control principle which based on hysteresis comparisons by selecting the optimum inverter switching modes. Generally, the Depenbrock upgraded the DTC control method and introduced the same technique with complex structures named DSC Figure 1.3 shows the DSC structure of induction motor.

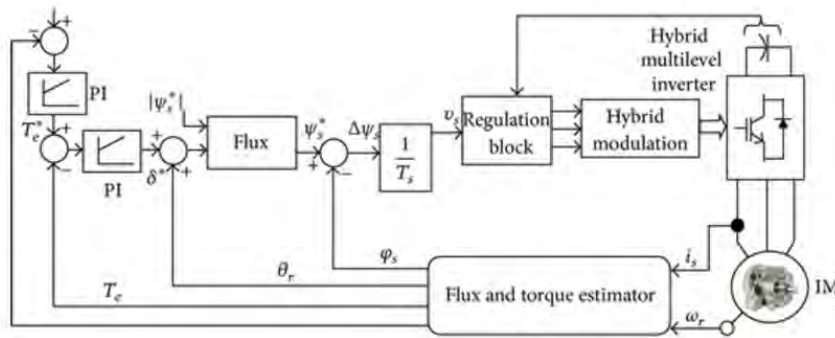


Figure 1.3 Structure of DSC of Induction Machine

Refers to the structure of the control method, DTC is the more simplicity compared to others. In fact, DTC is a fast instantaneous control performance. DTC is widely used and replaces the FOC for many industrial applications, while DSC is used for the high power drives. However, the DTC control method has major drawbacks such as larger torque ripple and variable switching frequency cause by the hysteresis operation in controlling the stator flux and torque.

Among the various modification of DTC, the Space Vector Modulation (SVM) was adapted in DTC structure has received widely acceptance. Due to SVM features can offer great reduction of torque ripple and a constant switching frequency (Mardani Borujeni and Ardebili, 2015, Bo et al., 2014, Tripathi et al., 2005, Lascu et al., 1992, Casadei et al., 1998). Although the implement of the SVM in DTC offers great reduction of torque ripple, but the present of the SVM increases the complexity which somehow degrades the accuracy of control performance and dynamic torque control performance.

Lately, the application of voltage source inverter has being popular and widely used to improve the DTC performances due to its attractive features such as low voltage stress on switching devices which allows to operate at high voltage or high current operations, low harmonic current or voltage distortion which eliminates the use of filter and improved efficiency and torque dynamic performance with optimal selection of voltage vectors.

## 1.2 Problem Statement

Direct Torque Control (DTC) is a simple method of controlling the torque and flux. Despite the simplicity, controlling induction motor by using DTC based on hysteresis controller will cause some major problem such as large torque ripple. Large torque ripple will increase the current as increased the current losses and lead to eddy current. However, by using the hysteresis controller, the torque can be adjusted to desired torque by changing the range of lower band and upper band. The middle of the band represented the torque reference or torque estimation. The band cannot be set too small because the incidents of overshoot in the estimated torque across the upper band in torque hysteresis band may occur and hence causes the reverse voltage vector to be selected. The selection reverse voltage vector causes torque decreased rapidly. The occurrence of torque changes rapidly will become more often and consequently produces larger torque ripple.

Although the torque ripple decreased, the switching frequency of the Voltage Source Inverter (VSI) will be increased. The rapidly increase of the switching frequency will cause heat at switching devices. The Integrated Gate Bipolar Transistor (IGBT) is being used as the switching devices. The heat produces will cause thermal losses. Furthermore, if the switching devices are withstanding the heat in a long period of time will affect the switching performance. The switching performance will be degraded due to thermal restriction.

### 1.3 Research Objective

The objective of this thesis to improve the performance of Direct Torque Control (DTC) of induction motor using Voltage Source Inverter (VSI) as the switching operation. The aim of this thesis is to reduce the torque ripple using the hysteresis-based torque controller. Next target of the project is to operate the switching devices, Integrated Gate Bipolar Transistor (IGBT) at optimal performance by replacing one switching device with a group of four switching device connected in parallel. Lastly, verify the technique and implement through simulation and experimentation result.

### 1.4 Project Scope

The scope of this project to conduct the proposed method to operate the induction motor with high performance. One of the scope of the project is to improve the Direct Torque Control (DTC) of induction motor performances by reducing the torque ripple using hysteresis-based controller. The other aim of the project is to ensure the switching operation is operating at optimal performance by replacing one switching device with a group of four switching devices connected in parallel in the structure of Voltage Sources Inverter (VSI). Lastly, the scope is to verify, evaluate and compare the improvements of the Direct Torque Control (DTC) method via simulations and hardware results.

## 1.5 Report Outline

This report consist of five chapters. This report starts with the introduction of the project, literature review, project methodology, result obtained, discussion and conclusion.

Chapter 1 covers the short explanation of project background, problem statement, objectives of the project and project scope.

Chapter 2 explains the basic operating principle of induction motor, short explanation of the control method and simple discussion about previous research of DTC of induction motor.

Chapter 3 covers the project methodology. This chapter consist of the mathematical model, flowchart of the project, milestone, Gantt chart, mapping of voltage vector selection, simulation model, switching operation of VSI, principle control of torque and flux and hysteresis operation.

Chapter 4 discusses the simulation results and hardware results then compare both results to verify the performances.

Chapter 5 is the summary of this project and recommendation for future work as to improve the performance of DTC of induction motor.

## CHAPTER 2

### LITERATURE RIVIEW

#### 2.1 Introduction

There are three major type of electric motor machine. The main types of electric motors are Direct Current (DC) motor, Alternating Current (AC) motor and special motor machine. The DC motors are divided into groups depend on their construction which are shunt, series, compound, separately-excited and switched reluctance motor. The AC motors are divided into two types respectively such as asynchronous motor and synchronous motor. Usually, all the machine will be connected with selected power converter types depends on the types of motor and the supply applied to the machines. There are four major types of power converter which are rectifier, chopper, inverter and cycloconverter. The three phase motors are motors designed to operate on three phase Alternating Current (AC) power used in many industrial applications. AC electricity changes direction from positive to negative and repeated many times as well as the motors are operating. AC change power in a smooth continuous wave called sine wave. The three phase AC has three sources of AC power with different phase angle to another. The phases are separated by  $120^\circ$  apart. There will be no two AC waves are ever at the same point at the same time. The important part in designing the construction of the motor is the controller. The basic function of the controller is to control the torque, flux or speed of the motor.

## 2.2 Asynchronous Motor

Asynchronous motor is an induction motor which is the motor most frequently and widely used in industry. Most of the induction motors are simple, rugged, low price and easy to maintain. The induction motors run at the constant speed from no load to full load. The speed is depending on the frequency respectively, therefore the induction motors are not easily adapted to speed control. However, there are some techniques can be used to control the operation of induction motor.

## 2.3 Operating Principle

The operation of a three phase induction motor is based upon the application of Faraday's Law and the Lorentz Force on a conductor. Consider a series of conductors of length,  $l$ , whose are short circuited by two bars. A permanent magnet placed above the conducting ladder, moves rapidly to the right at a speed,  $v$ , so that the magnetic field,  $B$ , sweep across the conductor. The sequence of events takes place:

1. By using Faraday's Law, a voltage  $E = Blv$  is induced in each conductor while being cut by the flux.
2. The induced voltage produces a current,  $I$ , which flow down the conductor underneath the pole-face, through the end-bars and back through the other conductor.
3. The current flow through conductor lies in the magnetic field of the permanent magnet, produces a mechanical force called Lorentz Force.
4. The force always acts in a direction to drag the conductor along with magnetic field.

If the conducting ladder is free to move, the rotor will accelerate towards the right. However, as control the speed, the conductors will be cut less rapidly by the moving magnet, with the result that the induced voltage,  $E$ , and the current,  $I$ , will diminish. In addition, the force acting on the conductors will also decrease. If the ladder were to move at the same speed as the magnetic field, the induced voltage,  $E$ , the current,  $I$ , and the force dragging the ladder along would all become zero.

## 2.4 Voltage Source Inverter (VSI)

The Voltage Source Inverter (VSI) can be divided into square wave inverter and Pulse Width Modulation (PWM) inverter is fed by a Direct Current (DC) source of very small internal resistance. VSI are basically built with Insulated Gate Bipolar Transistor (IGBT) or Gate Turn-Off (GTO) thyristor. Normally, the input voltage of the inverter will parallel with a capacitor to produce a constant DC voltage. The output terminal is an Alternating Current (AC) will remain constant irrespective of the load current drawn theoretically. Figure 2.1 shows the topology circuit of Voltage Source Inverter (VSI).

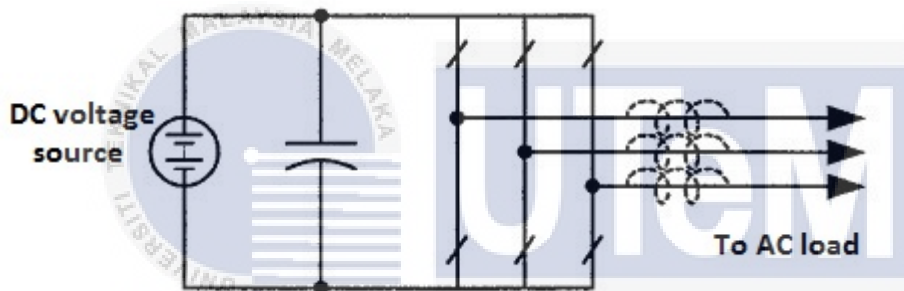


Figure 2.1: Topology Circuit of Voltage Source Inverter

## 2.5 Control Strategy of Induction Motor

The control method of induction motors can be classified into two groups named scalar control and vector control strategies. The scalar control method is based on two parameters simultaneously. The speed can be changed by varying the supply frequency. The impedance will be changing according to the operation of increasing or decreasing the supply frequency. In fact, the changes of the impedances will affect the current. If the supply frequency is decreasing or the voltage applied is increasing, the coils inside the induction motor can be burned or saturation in the iron of coils can occur. These problem can be avoided by using the scalar control. It is very necessary to control the frequency and vary the voltage simultaneously.

The vector control method is a principle which works with rotating vectors in a complex coordinate system. The phase voltage and the phase current will be changed. By using the vector control technique, it is possible to uncouple the field components. The uncoupling components established independent controlled current and single control currents which are the flux-producing current and the torque producing current. By using the established currents, the flux and the torque can be independently be controlled. In addition, the uncouple control currents are being separated by an angle of  $90^\circ$  apart from each other. As the conclusion, it is better to use the vector control method compared to scalar control technique as the complexity of the vector control method are less and high performance drive can be obtained.

### 2.5.1 Direct Torque Control (DTC)

Direct Torque Control (DTC) is one of the method that used in Variable Frequency Drives (VFD) generally to control the torque, as well as the speed of three phase Alternating Current (AC) motor. The DTC control method involves an estimation of the magnetic flux and torque of the motor depends on measured voltage and current of the motor. Integrate the stator voltages to estimate the stator flux linkage. The torque estimation due to the cross product of estimated linkage vector and the measured current vector of the motor. The estimated torque and the flux will be compared to the reference values respectively. If the estimated torque or estimated flux has a lot of differences from the reference values, the switching of the Voltage Source Inverter (VSI) will operate. So, the flux and torque will be in the tolerant band. The tolerant band is set in the hysteresis controller. Figure 2.2 shows the overview of torque and flux to be controlled.

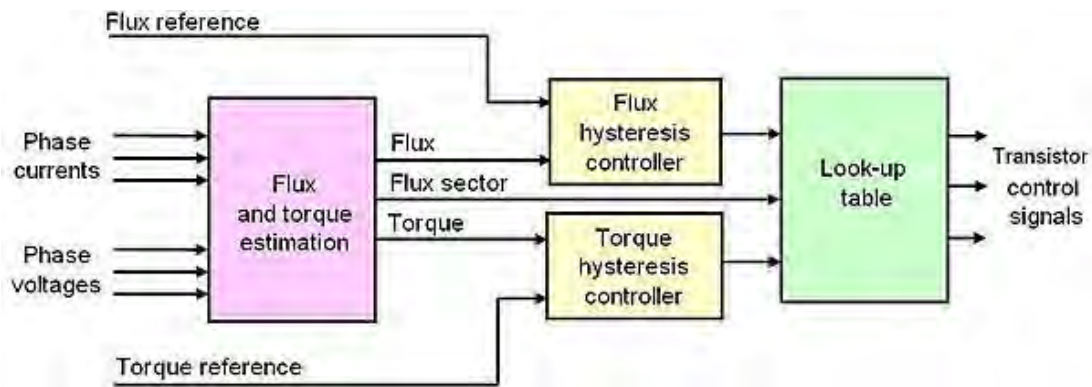


Figure 2.2: Overview of Torque and Flux Controller

Figure 2.3 shows the general structure of Direct Torque Control (DTC). The torque and flux reference values will be compared to the torque and flux estimation respectively. The torque and flux will be fed into the hysteresis controller to produce desired torque and flux. The look-up table is a table related to the switching operation of Voltage Source Inverter (VSI). The three phase voltage and current will be converted into two phase. The conversion of the phases is to make the voltage and current easier to estimate. The voltage and current is fed into the torque and flux estimator to produce estimated torque and flux as well as to detect the sector of flux.

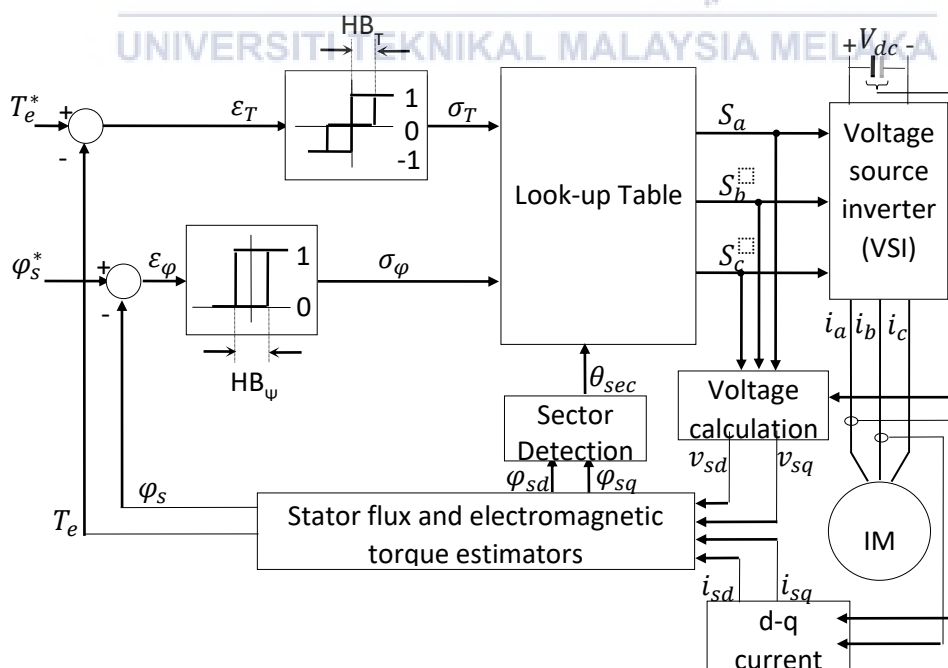


Figure 2.3: General Structure of Direct Torque Control

The inconsistencies torque ripple and rate of change of torque contribute to the raise of problems such as larger torque ripple and variable switching frequency. It should be noted that the rate of change of torque, either positive or negative torque slope varies according to motor operating conditions such as load torque and speed operations (Jun-Koo and Seung-Ki, 1999, Casadei et al., 1997).

## 2.6 Performance Improvements of Direct Torque Control

Several modifications on DTC structure or control algorithm were proposed to minimize the problems. Some of the proposed methods retain the simple structure of DTC with minor modifications on DTC structure (Noguchi et al., 1999, Jidin et al., 2011, Casadei et al., 1994b), while others employed modulation or different control techniques which somehow increase the complexity of the DTC structure (Habetler et al., 1992, Tripathi et al., 2005, Kumar et al., 2015). There are also some efforts utilized different topologies of inverters, e.g. the use of multilevel inverters (Alias et al., 2015, Rahim et al., 2015, Gholinezhad and Noroozian, 2012, Nordin et al., 2011).

There are several papers were proposed to overcome the problems and improve the DTC performance. The papers includes the improvement of flux estimation (Idris and Yatim, 2000, Bird and Zelaya De La Parra, 1996), sensor-less drive (Ma et al., 2013, Yongchang et al., 2012), torque capability for wide speed ranges (Jidin et al., 2012, Casadei et al., 2007), torque dynamic control in flux weakening region (Tripathi et al., 2006), reduction of torque ripple (Jidin et al., March 2011, Kumar et al., 2015, Yuan and Zhu, 2015) and provide a constant switching frequency (Habetler et al., 1992, Bo et al., 2014, Mardani Borujeni and Ardebili, 2015).

## CHAPTER 3

### RESEARCH METHODOLOGY

#### 3.1 Introduction

This chapter will be discuss the method of Direct Torque Control (DTC) of induction motor. The switching method of three phase Voltage Source Inverter (VSI) is used in order to complete project. The explanation included the topology circuit of VSI, the switching status and the constraint of using the method. At first, the mapping of voltage vectors on the  $d-q$  voltage vector plane will be presented to show the available of voltage vectors in the inverter. The selected voltage vector is depends on the switching sequence of the inverter. Desired torque slope can be produce by selecting the voltage vector. In this section, the principle control of flux and torque will be explained in detail. The torque and flux will be fed into a look-up table to select appropriate amplitude of voltage vector in selected sector.

### 3.2 Mathematical Modelling of Three Phase Induction Motor

It is necessary to develop mathematical modelling of induction machine that can be used to investigate the control behaviour of the motor under steady state and dynamic conditions. Basically, the induction machine involves complex equations due to three-phase quantities, nonlinear effects and mutual inductance coupling between the stator and rotor. However, the complex equations can be simplified by expressing the machine equations into space vector equations with some assumptions as listed below:

- Electrical machine configuration is symmetrical.
- The effect of harmonics of the stator and rotor magnetic flux is neglected.
- Infinity permeability iron
- Saliency effect, the slotting effects are ignored
- Voltage and current in sinusoidal term due to identical three-phase impedances or windings

Figure 3.1 shows a cross-section view of the symmetrical two poles of three-phase induction machine, which is drawn based on assumptions above. From this figure, it shows that there are two parts namely, stator and rotor parts. The stator has  $d$ -axis and  $q$ -axis which does not rotate, otherwise the rotor with the axis of  $d^r$ -axis and  $q^r$ -axis which rotates accordingly with respect to the rotor. It can be shown that the DTC computation uses all parameters or quantities, which are expressed with referring to the stator stationary reference frame.

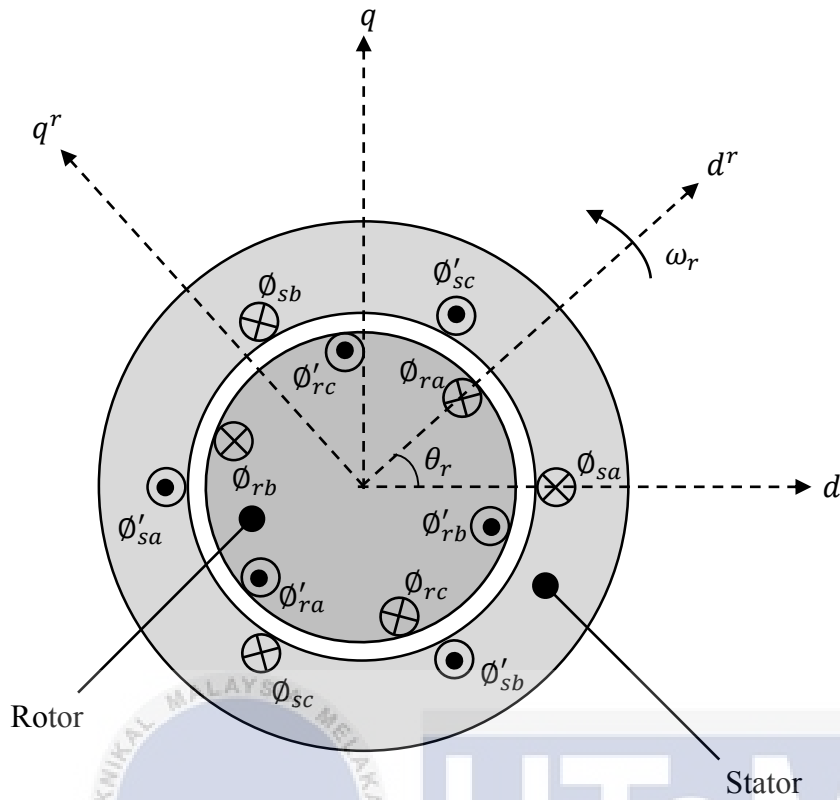


Figure 3.1: Cross Section of Single Pole Three Phase Motor

By considering the assumptions above, all machine equations can be simply expressed in term of space vectors. Meaning that, three phase variables such as three-phase current, voltage, magnetic motive force or flux can be written generally in a single space vector  $\bar{x}_s$  as given in (3.1).

$$\bar{x}_s = \frac{2}{3} [x_a + \bar{a}x_b + \bar{a}^2x_c] \quad (3.1)$$

where  $\bar{a} = e^{j120^\circ}$  is a unit vector. By employing space vector definition, all machine equations can be written into space vector form, referring to the stator stationary reference frame, as follows:

$$\bar{v}_s = R_s i_s + \frac{d\bar{\varphi}_s}{dt} \quad (3.2)$$

$$\bar{v}_r = R_r \bar{i}_r + \frac{d\bar{\varphi}_r}{dt} - j\omega_r \bar{\varphi}_r \quad (3.3)$$

$$\bar{\varphi}_s = L_s \bar{i}_s + L_m \bar{i}_r \quad (3.4)$$

$$\bar{\varphi}_r = L_r \bar{i}_r + L_m \bar{i}_s \quad (3.5)$$

$$T_e = \frac{3}{2} P \bar{\varphi}_s \times \bar{i}_s \quad (3.6)$$

All equations above, can be written into real and imaginary components or  $d$ - $q$  plane.

$$v_{sd} = R_s i_{sd} + \frac{d}{dt} \varphi_{sd} \quad (3.7)$$

$$v_{sq} = R_s i_{sq} + \frac{d}{dt} \varphi_{sq} \quad (3.8)$$

$$v_{rd} = R_r i_{rd} + \frac{d}{dt} \varphi_{rd} + \omega_r \varphi_{rq} \quad (3.9)$$

$$v_{rq} = R_r i_{rq} + \frac{d}{dt} \varphi_{rq} - \omega_r \varphi_{rd} \quad (3.10)$$

$$\varphi_{sd} = L_s i_{sd} + L_m i_{rd} \quad (3.11)$$

$$\varphi_{sq} = L_s i_{sq} + L_m i_{rq} \quad (3.12)$$

$$\varphi_{rd} = L_r i_{rd} + L_m i_{sd} \quad (3.13)$$

$$\varphi_{rq} = L_r i_{rq} + L_m i_{sq} \quad (3.14)$$

The stator and rotor voltage components as given in (3.7) to (3.10) can be written into a matrix form, as shown by (3.15):

$$\begin{bmatrix} v_{sd} \\ v_{sq} \\ v_{rd} \\ v_{rq} \end{bmatrix} = \begin{bmatrix} R_s s L_s & 0 & s L_m & 0 \\ 0 & R_s s L_s & 0 & s L_m \\ s L_m & \omega_r L_m & R_r + s L_r & \omega_r L_r \\ -\omega_r L_m & s L_m & -\omega_r L_r & R_r + s L_r \end{bmatrix} \cdot \begin{bmatrix} i_{sd} \\ i_{sq} \\ i_{rd} \\ i_{rq} \end{bmatrix} \quad (3.15)$$

where 's' represents the Laplace operator (as  $s \rightarrow d/dt$ ). By rearranging (3.15), the machine equation can be written into a state space form, where the stator and rotor currents are set as state variables, as given in (3.16) (P. Vas, 1992).

$$\begin{bmatrix} \dot{i}_{sd} \\ \dot{i}_{sq} \\ \dot{i}_{rd}' \\ \dot{i}_{rq}' \end{bmatrix} = \frac{1}{L_m^2 - L_s L_r} \begin{bmatrix} R_s L_r & -\omega_r L_m^2 & -R_r L_m & -\omega_r L_r L_m \\ \omega_r L_m^2 & R_s L_r & \omega_r L_r L_m & -R_r L_m \\ -R_s L_m & \omega_r L_m L_s & R_r L_s & \omega_r L_r L_s \\ -\omega_r L_m L_s & -R_s L_m & -\omega_r L_r L_s & R_r L_s \end{bmatrix} \begin{bmatrix} i_{sd} \\ i_{sq} \\ i_{rd}' \\ i_{rq}' \end{bmatrix} \\
+ \frac{1}{L_m^2 - L_s L_r} \begin{bmatrix} -L_r & 0 \\ 0 & -L_r \\ L_m & 0 \\ 0 & L_m \end{bmatrix} \begin{bmatrix} v_{sd} \\ v_{sq} \end{bmatrix} \quad (3.16)$$

For calculating the electromagnetic torque, the stator flux vector in (3.6) is substituted using (3.4), this yields

$$T_e = \frac{3}{2} P (L_s \bar{i}_s + L_m \bar{i}_r) \times \bar{i}_s \quad (3.17)$$

The stator current and rotor current vectors in (3.17) are written into  $d$ - and  $q$ -axis components, then by cross multiplying, the electromagnetic torque in terms of current components is obtained as,

$$T_e = \frac{3}{2} P L_m (i_{rd}' i_{sq} - i_{rq}' i_{sd}) \quad (3.18)$$

Where  $P$  is the number of pole pairs

Equations (3.16) and (3.18) are used to construct the mathematical modelling of a three-phase induction machine, which are valid for investigating motor or DTC performances under steady state and dynamic conditions.

### 3.3 Three Phase Voltage Source Inverter (VSI)

Basically, inverter is a term that known as a way to convert Direct Current (DC) to Alternative Current (AC). The VSI is fed from a DC voltage source and the input voltage is remain constant. The output voltage of the does not depends on the load. The waveform of the load current as well as its magnitude depends upon the nature of load impedance.

#### 3.3.1 Topology Circuit of VSI

The three phase Voltage Source Inverter (VSI) contain six number of Insulated Gate Bipolar Transistor (IGBTs) where each leg is made up by a pair of power switching devices. The pair of power switching devices must be vice versa to one another in each leg. Every legs are complimentary to one another on operation. There is a short circuit if the pair of power switching devices in a leg is ON at the same time. For example, when the voltage is supplied to the VSI circuit, if the upper switch ( $S_a$ ) is ON, it is compulsory for the lower switch ( $\bar{S}_a$ ). Figure 3.2 shows the topology circuit of VSI. Leg1 represents phase A, Leg2 represented phase B and Leg3 represented phase C.

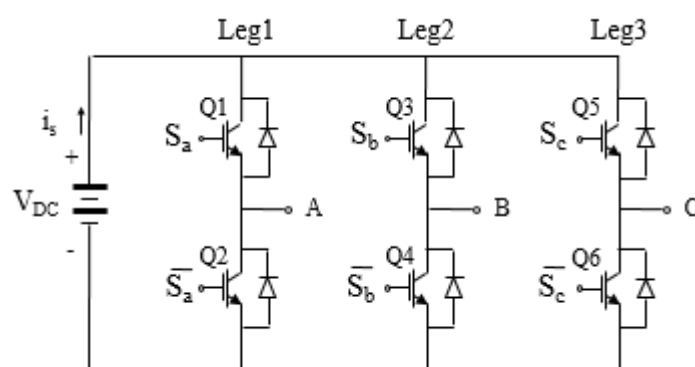


Figure 3.2: Topology Circuit of Voltage Source Inverter

The topology circuit is simplified to make easier to understand. Q1 and Q2 are a pair of power switching devices in Figure 3.1. The both IGBTs in the leg are replaced by a switch. The switch represented the power switching devices. Figure 3.3 shows the simplified topology circuit of Voltage Source Inverter (VSI). The definition of switching status at each leg as shown below.

$$S_x = \begin{cases} 1 & \text{upper IGBT ON} \\ 0 & \text{lower IGBT ON} \end{cases}$$

Where x represented as a, b and c

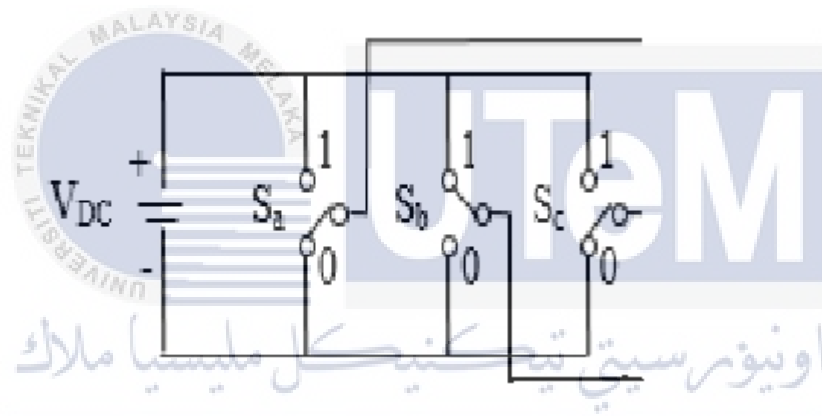


Figure 3.3: Simplified Voltage Source Inverter Circuit

### 3.3.2 Mapping of Voltage Vector

In generally, there are eight combinations of switching state from the equation  $2^n$ , where n is the number of phase can be obtain in the three phase VSI. The Figure 3.4 shows the eight possibilities of switching state including their voltage vectors on the voltage vector  $d$ - $q$  plane. In the figure below, the x-axis is replaced by  $d$ -axis while y-axis is replaced by  $q$ -axis. Two of eight voltage vectors are categorized as zero voltage vectors and located at origin which are  $\bar{v}_0$  and  $\bar{v}_7$  while the rest of six voltage vectors is categorized as active voltage vector.

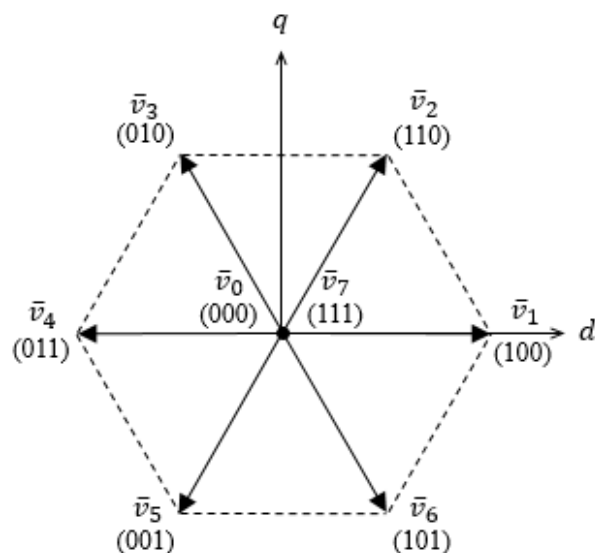


Figure 3.4: Voltage Vectors with Switching Status in VSI

### 3.3.3 Clarke Transformation

Clarke transformation is a space vector transformation of time-domain signals from a natural three phase coordinate system into a stationary two phase reference frame. Figure 3.5 shows the sinusoidal waveform of the three phase with the same corresponding magnitude and Figure 3.6 shows the different angles between each phase.

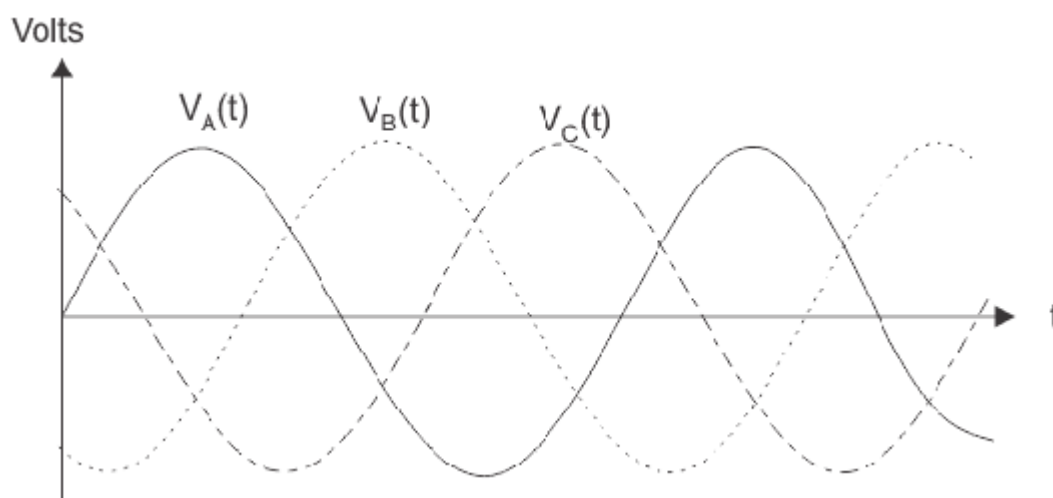


Figure 3.5: Three Phase Sinusoidal Waveform

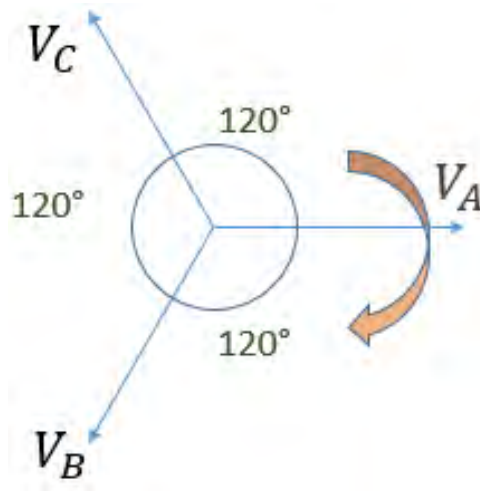


Figure 3.6: Voltage Vector of Three phase

From the figures above, obtain the equation of the three phase in matrix form as shown below.

$$\begin{bmatrix} V_A \\ V_B \\ V_C \end{bmatrix} = \begin{bmatrix} V_m \cos(\omega t) \\ V_m \cos\left(\omega t + \frac{2\pi}{3}\right) \\ V_m \cos\left(\omega t - \frac{2\pi}{3}\right) \end{bmatrix} \quad (3.19)$$

$$T_{\alpha\beta 0} = T_{dq0} = \frac{2}{3} \begin{bmatrix} 1 & -1/2 & -1/2 \\ 0 & \sqrt{3}/2 & -\sqrt{3}/2 \\ 1/2 & 1/2 & 1/2 \end{bmatrix} \quad (3.20)$$

By referring the equation of Clarke Transformation, state as shown below.

$$\begin{bmatrix} V_d \\ V_q \\ V_0 \end{bmatrix} = T_{dq0} \begin{bmatrix} V_A \\ V_B \\ V_C \end{bmatrix} \quad (3.21)$$

By substitute the equation (3.19) and (3.20) in Clarke Transformation equation (3.21)

$$\begin{bmatrix} V_d \\ V_q \\ V_0 \end{bmatrix} = \frac{2}{3} \begin{bmatrix} 1 & -1/2 & -1/2 \\ 0 & \sqrt{3}/2 & -\sqrt{3}/2 \\ 1/2 & 1/2 & 1/2 \end{bmatrix} \begin{bmatrix} V_m \cos(\omega t) \\ V_m \cos\left(\omega t + \frac{2\pi}{3}\right) \\ V_m \cos\left(\omega t - \frac{2\pi}{3}\right) \end{bmatrix} \quad (3.22)$$

Solve the equation (3.22) will obtain the two phase voltages which are  $V_d$  and  $V_q$  as follows.

$$\begin{bmatrix} V_d \\ V_q \\ V_0 \end{bmatrix} = \begin{bmatrix} V_m \cos(\omega t) \\ V_m \sin(\omega t) \\ 0 \end{bmatrix} \quad (3.23)$$

Cartesian axes are also portrayed, where  $V_d$  is the horizontal axis aligned with phase  $V_A$  and the vertical axis rotated by  $90^\circ$  is indicated by  $V_q$ . Both phase voltages have the same magnitude. Figure 3.7 shows the two phase voltage produce by the Clarke transformation. The red colour waveform refers the phase voltage of  $V_d$  while the blue colour waveform presents the phase voltage of  $V_q$ . The magnitude of phase are proven same.

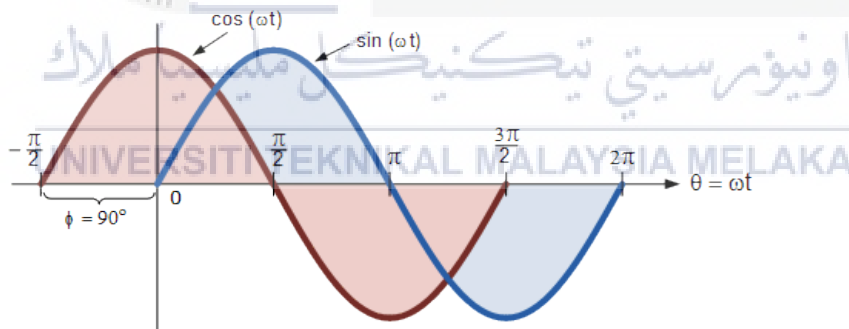


Figure 3.7: Two Phase Voltage

The three phase rotor and stator voltage equation can be written into a matrix form and transform into two phase rotor and stator voltage equations by using Park's Transformation. The transformation equation used by assume the balanced three phase voltage with the angle of  $120^\circ$  apart from each phase. The three phase stator voltage are presented by  $V_{As}$ ,  $V_{Bs}$ ,  $V_{Cs}$ , and will be transformed into two phase stator voltage which are notated as  $V_{sd}$  and  $V_{sq}$ . The magnitude of the two phase voltages are will be

assumed as 1V and the axes of two phase voltage are oriented at an angle of  $\theta$ . Finally, the equation is written in matrix form as shown below.

$$\begin{bmatrix} V_{As} \\ V_{Bs} \\ V_{Cs} \end{bmatrix} = \begin{bmatrix} \cos \theta & \sin \theta & 1 \\ \cos(\theta - 120^\circ) & \sin(\theta - 120^\circ) & 1 \\ \cos(\theta + 120^\circ) & \sin(\theta + 120^\circ) & 1 \end{bmatrix} \begin{bmatrix} V_{sd} \\ V_{sq} \\ V_{s0} \end{bmatrix} \quad (3.24)$$

Inverse the equation (3.24) will obtain the equation as follows.

$$\begin{bmatrix} V_{sd} \\ V_{sq} \\ V_{s0} \end{bmatrix} = \frac{2}{3} \begin{bmatrix} \cos \theta & \cos(\theta - 120^\circ) & \cos(\theta + 120^\circ) \\ \sin \theta & \sin(\theta - 120^\circ) & \sin(\theta + 120^\circ) \\ 0.5 & 0.5 & 0.5 \end{bmatrix} \begin{bmatrix} V_{As} \\ V_{Bs} \\ V_{Cs} \end{bmatrix} \quad (3.25)$$

Where  $V_{s0}$  is added as the zero sequence component, which may or may not be present. So, the zero sequence component and be neglected. If the  $\theta$  is set to zero and the two phase voltage will be obtained as the equations (3.26) and (3.27) as shown below.

$$V_{sd} = \frac{2}{3} \left( V_{As} - \frac{1}{2} V_{Bs} - \frac{1}{2} V_{Cs} \right) \quad (3.26)$$

$$V_{sq} = \frac{2}{3} \left( V_{As} - \frac{1}{2} V_{Bs} - \frac{1}{2} V_{Cs} \right) \quad (3.27)$$

### 3.4 Estimation of Torque and Flux

Recently, Direct Torque Control (DTC) has becoming a promising alternative solution to high performance vector control technique for induction motor drives. Compared to the Field Oriented Control (FOC), DTC has a very simple structure, does not require current regulators, and in principle does not require a speed sensor to operate. The performance of DTC drive very much depends on the accuracy of the estimated electromagnetic torque and stator flux linkage based on the terminal variables of the machine, such as the stator currents and voltages. In general, the flux linkage vector can be estimated either based on the voltage model, or the current model equations. However, it turns out that the estimation of the stator flux linkage using voltage model normally has problems at low speed operations. Stator flux can be estimated using stator voltage equation as given in (3.2). Rearrange the equation of (3.2) as shown below.

$$\frac{d\bar{\varphi}_s}{dt} = \bar{v}_s - R_s i_s \quad (3.28)$$

By integrating the both side of the equation (3.28), stator flux will obtain as shown in equation (3.29)

$$\int \frac{d\bar{\varphi}_s}{dt} = \int (\bar{v}_s - R_s i_s)$$

$$\bar{\varphi}_s = \int (\bar{v}_s - R_s i_s) dt \quad (3.29)$$

The stator flux in equation (3.29) can be expressed in term of  $d$ - $q$  axis.

$$\bar{\varphi}_{sd} = \int (\bar{v}_{sd} - R_s i_{sd}) dt \quad (3.30)$$

$$\bar{\varphi}_{sq} = \int (\bar{v}_{sq} - R_s i_{sq}) dt \quad (3.31)$$

### 3.5 Principle Control of Torque and Flux

The torque and flux are being controlled in Direct Torque Control (DTC) to ensure the high performance of the induction motor. This section will discuss the principle control of torque and stator flux by using hysteresis controller and selection of voltage vector. The explanation included the hysteresis controller operation, controlling the torque and the flux.

### 3.5.1 Hysteresis Controller

A hysteresis controller is a simple controller to control the desired output in between the tolerant band. In this project, hysteresis controller is used to maintain the torque and the flux follows the reference torque. The reference torque and flux must be set as suitable and desired torque and flux. The hysteresis controller has to set the limit for the Upper Band (UB) and Lower Band (LB). The hysteresis controller has its own level to be set. The torque is controlled using the three level hysteresis controller while the flux is controlled using the two level hysteresis controller. The difference between both levels is the band. The three level must be set UB and LB limit whereas the two level just set for UB limit only where the LB is zero.

The concept of hysteresis controller operation is basically simple. If the torque or the flux values reaches at the UB that being set earlier, it will be decreased until the torque or the flux until the values reaches the LB value. It will get better result as the band become smaller. Theoretically, the smaller the band, the output will follows the reference smoothly but there are some problems need to be considered such as frequency. Figure 3.8 demonstrates the simple operation of hysteresis controller.

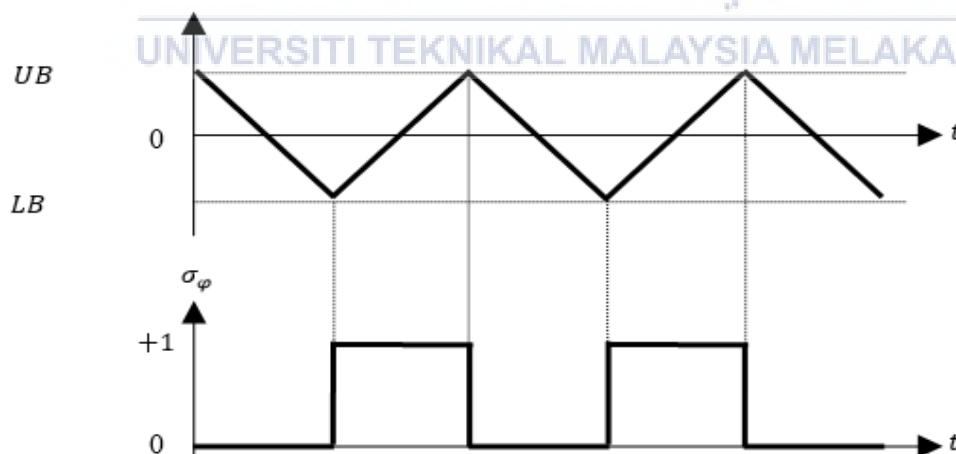


Figure 3.8: Operation of Hysteresis Controller

### 3.5.2 Control of Torque

The principle of controlling the torque can be describe by rearrange the torque equation (3.6) and express the equation in terms of stator flux and rotor flux vectors. The equation will produced as given in the equation (3.32).

$$T_e = \frac{3}{2} P \frac{L_m}{\sigma L_s L_r} |\bar{\varphi}_s| \cdot |\bar{\varphi}_r| \sin \delta_{sr} \quad (3.32)$$

Where,  $\delta_{sr}$  is the different angle between the vectors of stator flux,  $\bar{\varphi}_s$  and rotor flux,  $\bar{\varphi}_r$ . The symbol  $\sigma$  in the torque equation represent the total leakage factor. The total leakage factor can be expressed as shown in equation (3.33).

$$\sigma = 1 - \frac{L_m^2}{L_s L_r} \quad (3.33)$$

Based on the equation (3.33), it proves that the variation of torque can be determined by the load angle,  $\delta_{sr}$  where assumed the magnitudes of stator flux and rotor flux vectors are constant.

Figure 3.9 describes the variations of load angle,  $\sigma$  increasing, decreasing and sharply decrease where the capability for the variations of load angle in application of vectors in Direct Torque Control (DTC). The rotor flux is being assumed to rotate anti-clockwise continuously at uniform and constant speed, while the stator flux will rotate with different instantaneous angular frequency. The irregular motion of stator flux will affect the change of the load angle. The Figure 3.8 shows the tendency of the load angle to increase, decrease or decrease sharply according to the torque error status that produced from the three level hysteresis controller.

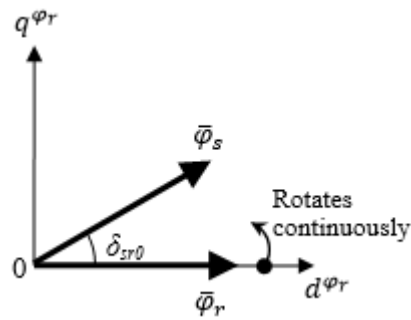


Figure 3.9: Stator and Rotor Flux Vector

The torque must be increased as the output of the torque hysteresis controller reaches the Upper Band (UB). This operation refers the torque error where the torque error is produced by comparing the torque reference and torque produced. The torque error should be reduced to prevent the torque error become larger. Hence, the suitable of active voltage vectors must be selected in order to increase the load angle as well as the torque. The selection of active voltage vectors instantly rotates the stator flux with higher angular frequency and greater load angle,  $\delta_{sr}$ . Figure 3.10 shows the load angle increased.

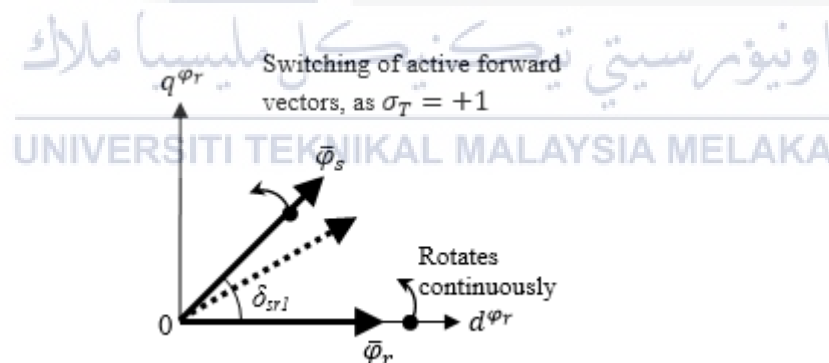


Figure 3.10: Active Forward Voltage Vectors

Sometimes, the torque needs to be decreased as the output of the torque hysteresis controller reaches the Middle Band (MB). This happen when the output of the torque reaches the desired torque reference. So, the selection of the voltage vector must be zero vectors to stop the stator flux moving further apart from the rotor flux. The zero vectors need to be selected as to prevent the load angle become larger. As mentioned above, the rotor flux vector keeps rotating with a constant speed. So, the

rotor flux vector will move approaching to the stator flux. In fact, the torque reduces as the load angle reduces. Figure 3.11 shows the torque error reaches MB.

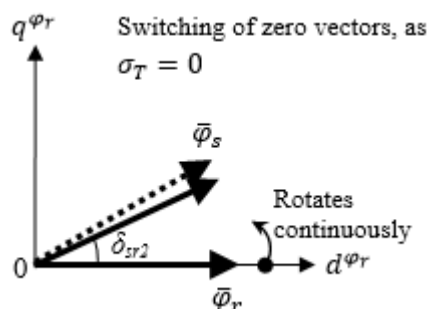


Figure 3.11: Zero Voltage Vectors

In other case, the torque needs to be reduced immediately, especially when the torque demand suddenly reduced for large amount. In this case, the torque error reaches the Lower Band (LB) and it is necessary to reduce the torque extremely. This situation can be solved by selecting the active reverse voltage vectors so the stator flux vector will rotate clockwise while the rotor flux vector keeps its constant speed and rotates as usual (anti-clockwise). By reducing the torque extremely, the torque error will increase sharply. The reduction of load angle might be a negative value, if the reference torque changed immediately. Figure 3.12 shows the selected reversed voltage vectors.

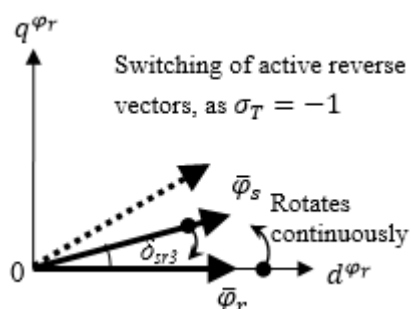


Figure 3.12: Active Reverse Voltage Vectors

Figure 3.13 shows the three level hysteresis controller while the Figure 3.14 shows the typical waveforms of torque control in Direct Torque Control (DTC) using hysteresis based controller.

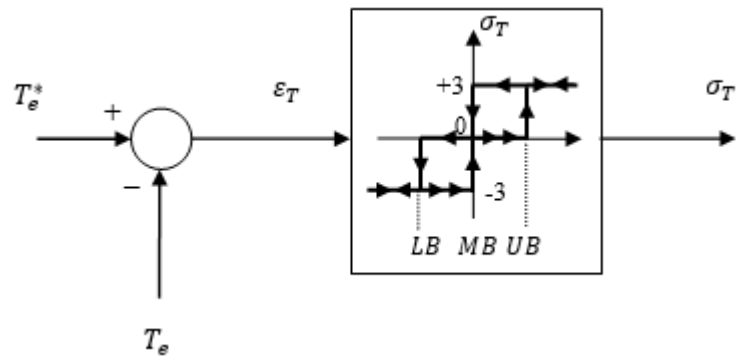


Figure 3.13: Three Level Hysteresis Controller

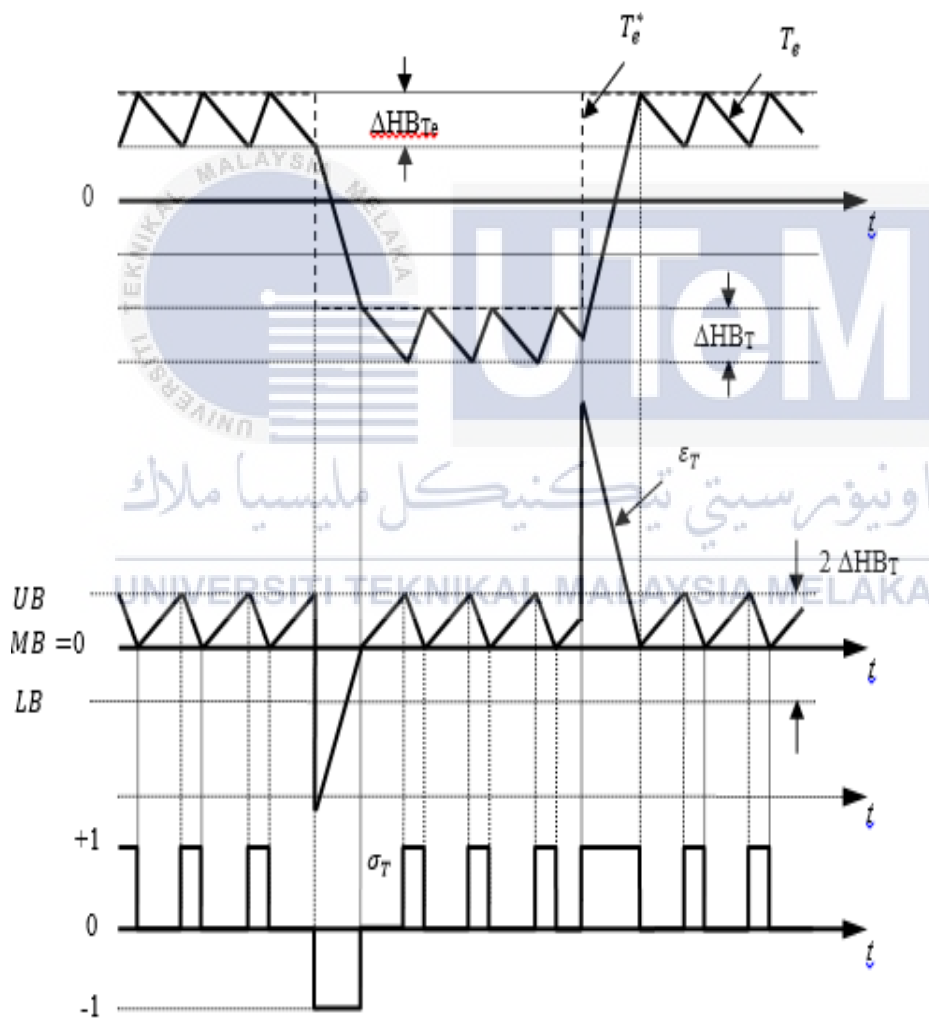


Figure 3.14: Typical Waveform of Torque, Torque Error &amp; Torque Status

### 3.5.3 Control of Stator Flux

By solving the equation of stator flux (3.29), where the voltage drop through the resistor can be neglected as the value is too small. The stator flux motion can be described as shown in the equation (3.34).

$$\Delta \bar{\varphi}_s = \bar{v}_s \cdot \Delta t \quad (3.34)$$

Equation (3.34) proves the stator flux motion is directly proportional to the applied voltage vectors.

The principle of flux control can be explained based on trajectory of stator flux with six divided sector as illustrated in Figure 3.15. By using Direct Torque Control (DTC), the stator flux trajectory is being controlled by controlling the radial component of stator by forming a circular locus. The stator flux is being by using two level hysteresis controller. The stator flux vector is controlled within a tolerant Upper Band (UB) and Lower Band (LB). The locus of the flux is controlled to be centred at the origin and the flux rotates anti-clockwise.

In Figure 3.15, the dashed line represent the circular reference and the magnitude stator flux vector is regulated to the track. There are two possible voltage vectors are used in order to control the stator flux in every sectors. These two voltage vectors is being selected as the voltage vector are the most tangential to the stator flux vector. Figure 3.15 shows the stator flux vector lies on the sectors II. So, the suitable voltage vectors for the sectors II are  $\bar{v}_2$  and  $\bar{v}_3$ . The voltage vectors are selected because the voltage vectors are the most tangential to the stator flux vector. For example,  $\bar{v}_2$  is tangential to the stator flux at boundaries between sector I and sector II while the voltage vector  $\bar{v}_3$  is tangential to the stator flux vector at the boundaries between sector II and sector III. In this sector, the voltage vector  $\bar{v}_2$  is used to increase the stator flux while the voltage vector  $\bar{v}_3$  is selected to decrease the stator flux. The locus of stator flux will seem more circular if the band of hysteresis controller is

reduced. In addition, it will produce lower current harmonic distortion. However, reducing the hysteresis band will increase the switching frequency of the inverter.

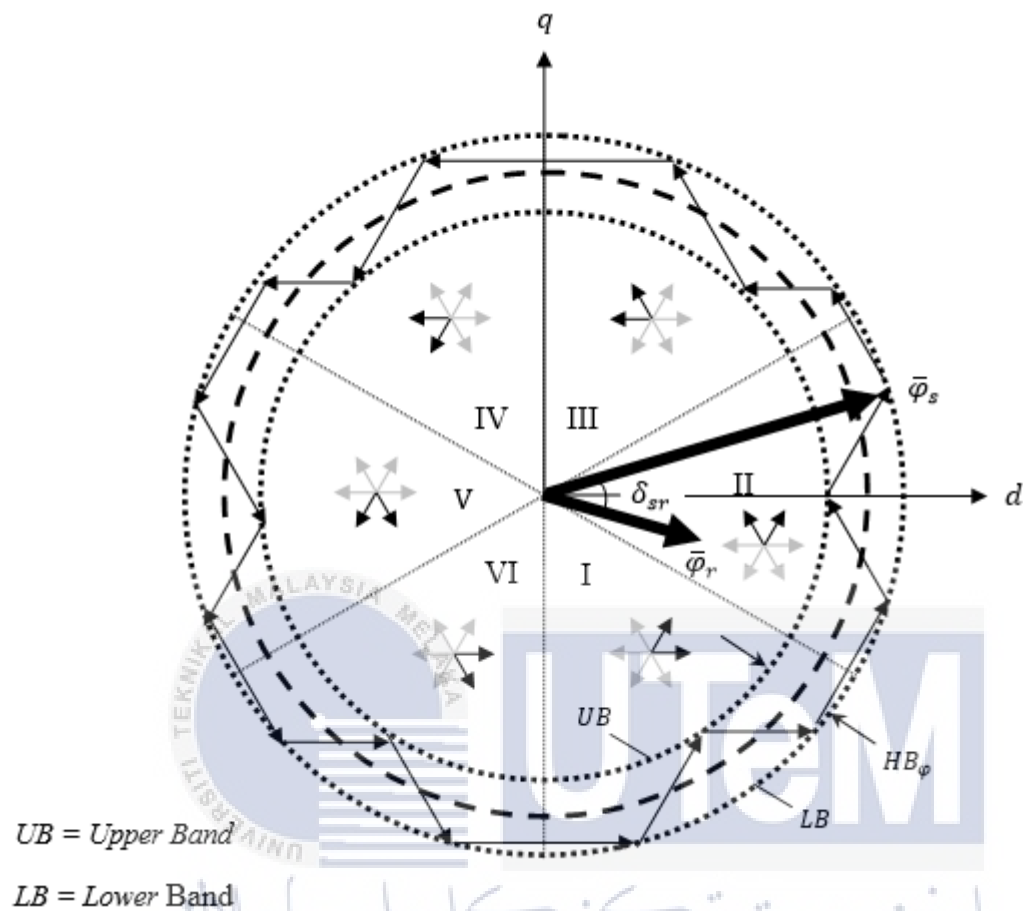


Figure 3.15: Trajectory of Stator Flux

In Direct Torque Control (DTC) scheme, the trajectory of stator flux to form a circular locus can be accomplished by controlling the radial or magnitude of stator flux vector using a two-level hysteresis controller, as shown in Figure 3.16. The hysteresis controller will produce two digitized output status,  $\sigma_\phi = +1$  or  $0$ ; i.e.  $\sigma_\phi = +1$  once the decrement of flux error touches the Lower Band (LB), while  $\sigma_\phi = 0$  once the increment of flux error reaches the Upper Band (UB). The production of output status from the hysteresis controller is used to select the appropriate vector to restrict the error within the hysteresis band, as shown in Figure 3.17. The selection of vector also requires flux sector information and output status from the torque hysteresis controller.

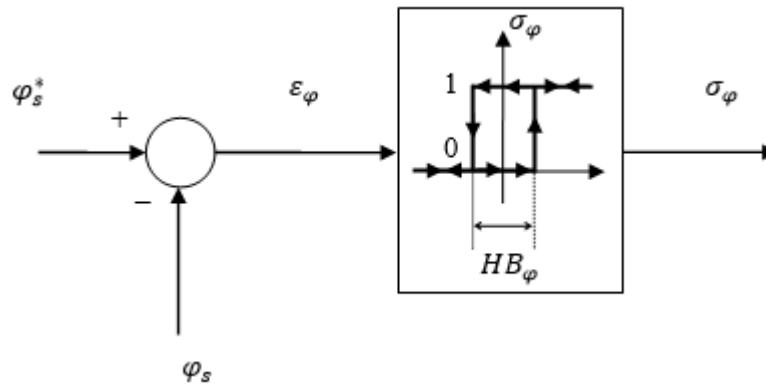


Figure 3.16: Two Level Hysteresis Controller

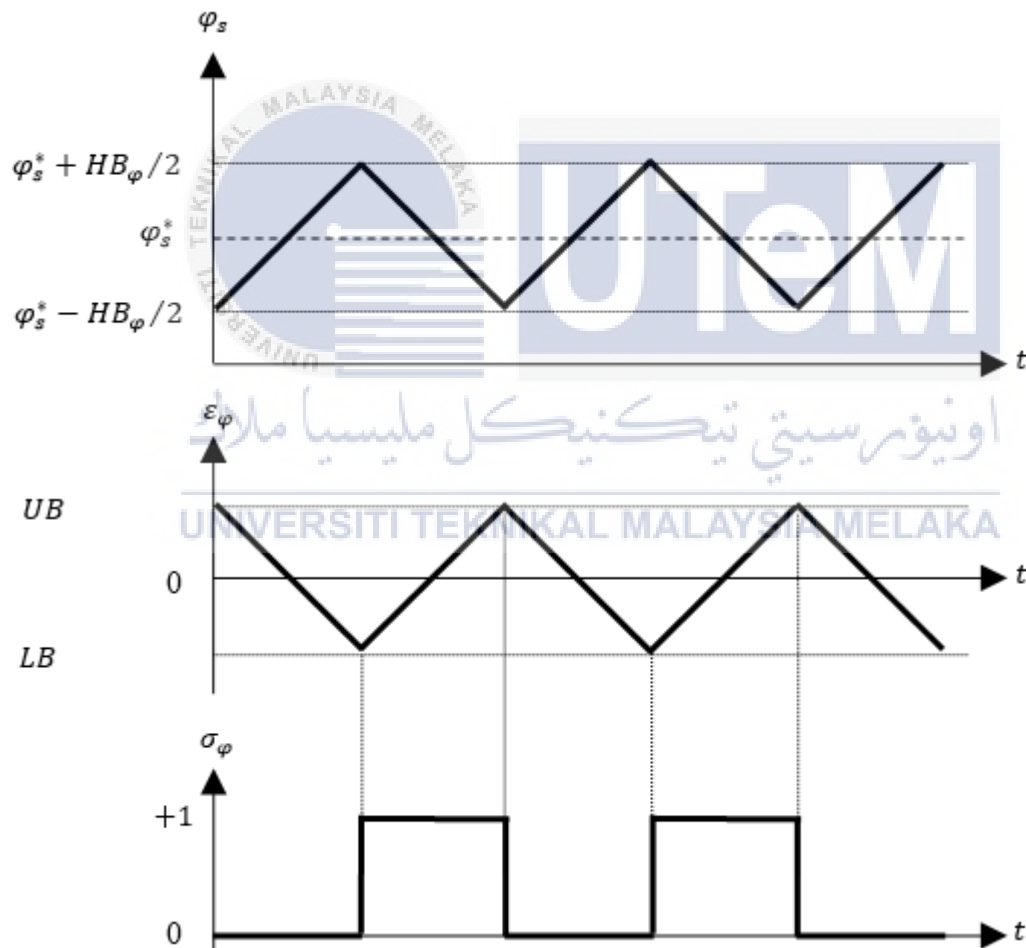


Figure 3.17: Typical Waveform of Stator Flux, Flux Error &amp; Flux Error Status

### 3.6 Sector Detection

The sector detection is one of the important operation in Direct Torque Control (DTC). As mentioned above the sector is divided into six sector where each sector has two suitable voltage vectors. The most tangential voltage is the most suitable voltage vectors according to the sector has been selected respectively. The sector can be recognized by the determining the stator flux vector. The stator flux vector rotates anti-clockwise as the locus of the stator flux vector is lies on the origin in  $d-q$  planes. The sector selection is used to detect the position of the stator flux vector. So, the suitable voltage vector easily to identify as the position of the stator flux vector as well as the torque error status and flux error status. The voltage vector then will transfer the information to the Voltage Source Inverter (VSI) which switching should be ON and OFF. For example, the VSI implemented in this project has three legs. The legs are expressed by binary number in Table 3.1. [leg1 leg2 leg3] is shown in the look-up table. The operation of VSI has been explained above. The information are concluded in look-up table as shown below.

Stator flux error status, $\sigma_\phi$	Torque error status, $\sigma_T$	Sector					
		I	II	III	IV	V	VI
1	+1	[100]	[110]	[010]	[011]	[001]	[101]
	0	[111]	[111]	[000]	[000]	[111]	[000]
	-1	[001]	[101]	[100]	[110]	[010]	[011]
0	+1	[110]	[010]	[011]	[001]	[101]	[100]
	0	[000]	[000]	[111]	[111]	[000]	[111]
	-1	[011]	[001]	[101]	[100]	[110]	[010]

Table 3.1: Look-up Table

### 3.7 Complete Circuit of Direct Torque Control of Induction Motor

Figure 3.18 shows the complete simulation circuit based hysteresis controller of Direct Torque Control (DTC) of induction motor (asynchronous motor). The torque reference and flux reference are fed into three level hysteresis controller and two level hysteresis controller respectively. The torque reference and flux reference is being compared to the torque error and flux error. Then, the torque error status and the flux error status will transfer the information to look-up table.

The information of three phase voltage is being convert into two phase. The Figure 3.19 shows the mathematical operation of the phase conversion. The 1<sup>st</sup> leg and 2<sup>nd</sup> leg currents is being convert into the  $d-q$  components by using the park transformation. The Figure 3.20 shows the mathematical modelling for the conversion of current components. The voltages and currents in form of  $d-q$  components are being calculated to produce estimation of torque and estimation of flux to be compared with torque and flux respectively. The mathematical expression is shown in Figure 3.21. From the calculated values, it is also produce the position of the flux stator in term of angle. By identifying the angle of flux stator, the stator flux vector can be recognized the sector easily.

By collecting the information of the torque error status, flux error status and the position of the stator flux vector, the switching of the Voltage Source Inverter (VSI) can be determined. The switching operation is depends on the information given. Then, the VSI will be fed to the induction motor. The motor will operation simultaneously with the produced switching frequency.

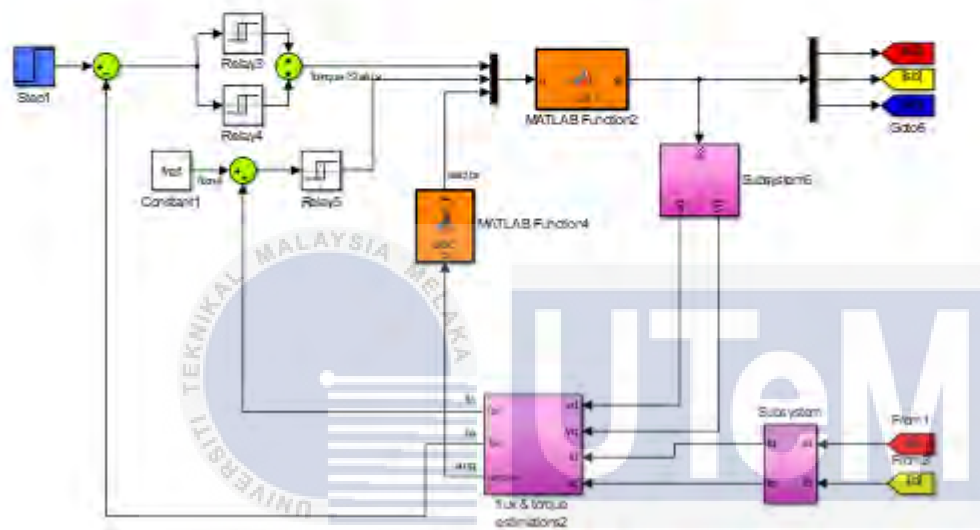
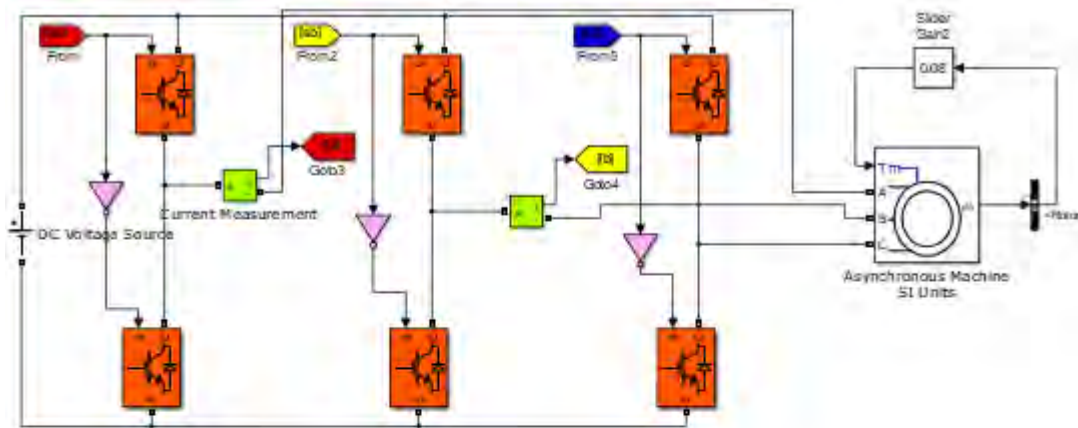


Figure 3.18: Complete Simulation Circuit of DTC  
 اونیورسیتی تکنیکل مالیزیا ملاک  
 UNIVERSITI TEKNIKAL MALAYSIA MELAKA



Figure 3.19: Mathematical Modelling for Voltage Components

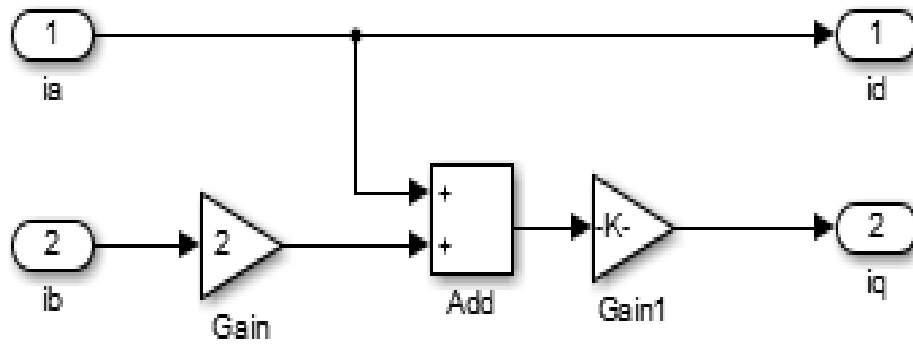


Figure 3.20: Mathematical Modelling for Current Components

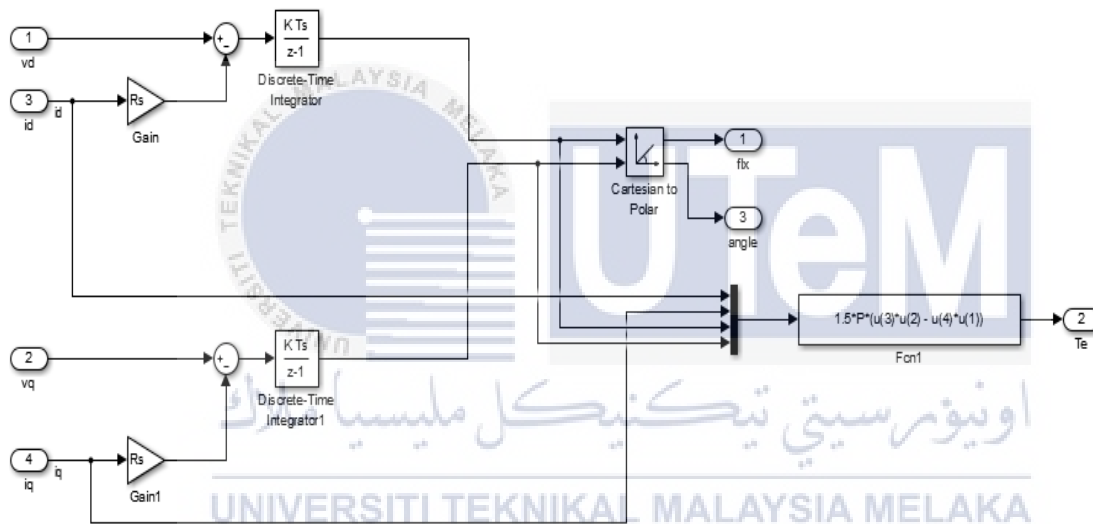


Figure 3.21: Expression of Estimation Torque, Estimation Flux and Angle

### 3.8 Proposed Technique

In this section, the explanation about the improvement of the control strategy using Direct Torque Control (DTC) of induction motor. Basically, the general concept of the DTC using hysteresis based controller is being used. The DTC operation has been explained above. The DTC is one of the simple structure of vector control method. However, using the DTC will produce high torque dynamic which means high efficiency. One of the advantage of using DTC control method is not required information of parameters of the induction motor.

The improvement is being done at the hysteresis controller. Reduced the Upper Band (UB) and Lower Band (LB) will increase the efficiency of the motor as the torque error will reduce and follow the reference torque as desired. However, this improvement leads to another problem. By reducing the hysteresis band, the switching frequency will become faster. This method will cause the degraded of switching operation as the switching devices need to withstand the high switching frequency. If the switching devices operate rapidly will cause heat on the body of the switching devices. So, it will cause thermal losses.

To solve the problem, the flexible and high performance of switching devices needs to be considered. The requirements will ensure really high cost of switching devices. Maybe the switching devices difficult to find in the market. The proposed technique is reduced the tolerant band of hysteresis controller and provide a numbers of switching devices. This technique to ensure the used switching devices can operate normally as to reduce the thermal losses cause by voltage drop across the switching devices. By implement a group of four switching devices as shown in figure below, the switching devices will have some times to rest. This method to ensure the switching devices operate at optimal performance and high efficiency. In fact, the thermal losses can be reduced. The figure below shows the proposed technique of DTC of induction motor using hysteresis based controller. The hysteresis band has been reduced technically.

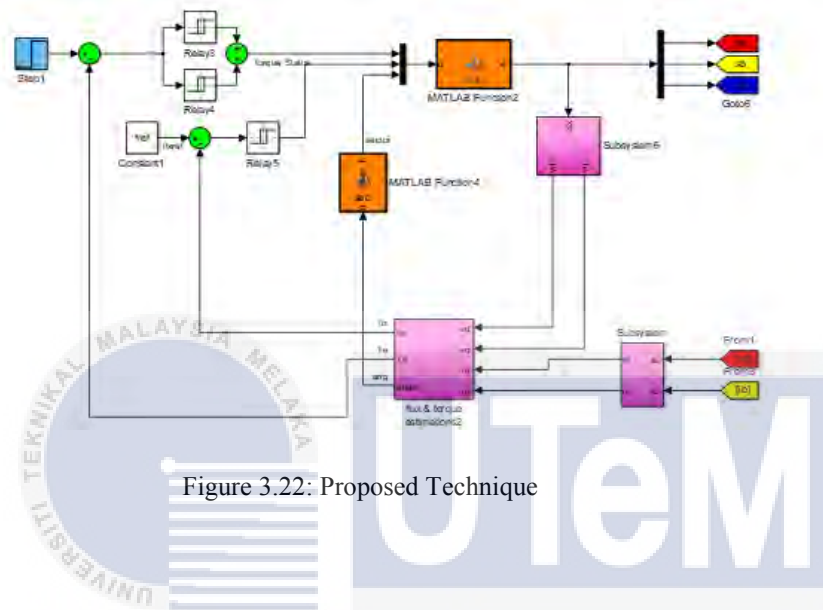
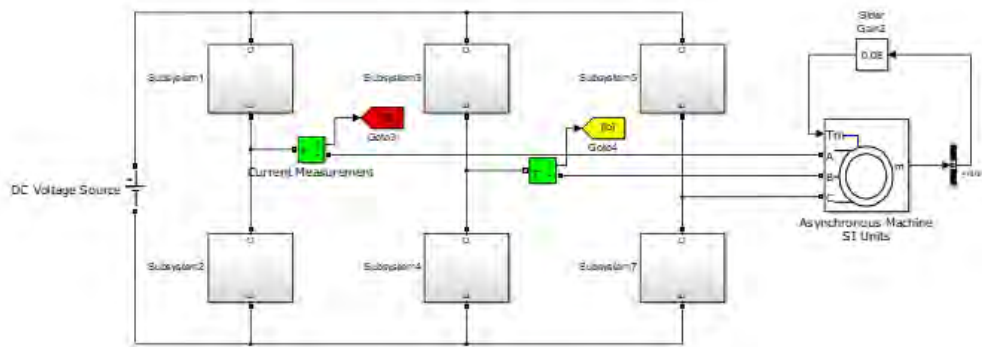


Figure 3.22: Proposed Technique

The proposed technique using the same vector control and operation. The circuit has been modified to improve the efficiency of the DTC performance. Figure 3.23 shows the group of four switching devices have been implemented in the circuit. The switching devices are connected parallel inside the subsystems available in the Voltage Source Inverter (VSI). Different signal will be injected to each of the switching device respectively.

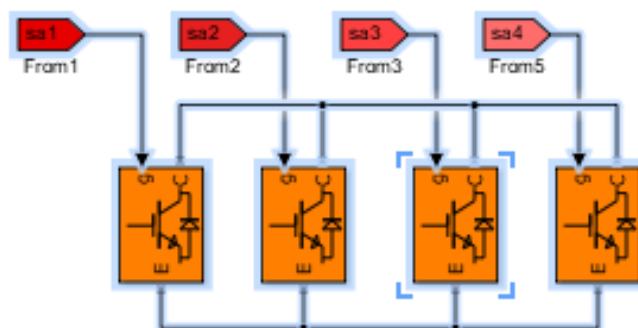


Figure 3.23: Group of Four Switching Devices

### 3.9 Hardware Implementation

The topics will explain the flow of hardware implementation. In order to complete the project, there are some procedures and guidelines need to follow. In theoretical, the Voltage Source Inverter (VSI) has three legs operate synchronously. Figure 3.24 shows the proposed structure of VSI. Each legs has upper side and lower side switching devices. Both sides must operate contradictory. In order to avoid the upper and lower side turn on simultaneously, blanking time effect must be implemented in switching operation. The generated signals from Dspace will feed into Dspace connector as shown in Figure 3.25. DSpace is an open source repository software package typically used for creating open access repositories for scholarly and/or published digital content. The signals will be sent to the FPGA to reconstruct the signals according to VHDL code. Lastly, the signals will be injected into the gate driver to operate the IGBT as well as the Voltage Source Inverter (VSI).



Figure 3.24: Structure of Voltage Source Inverter

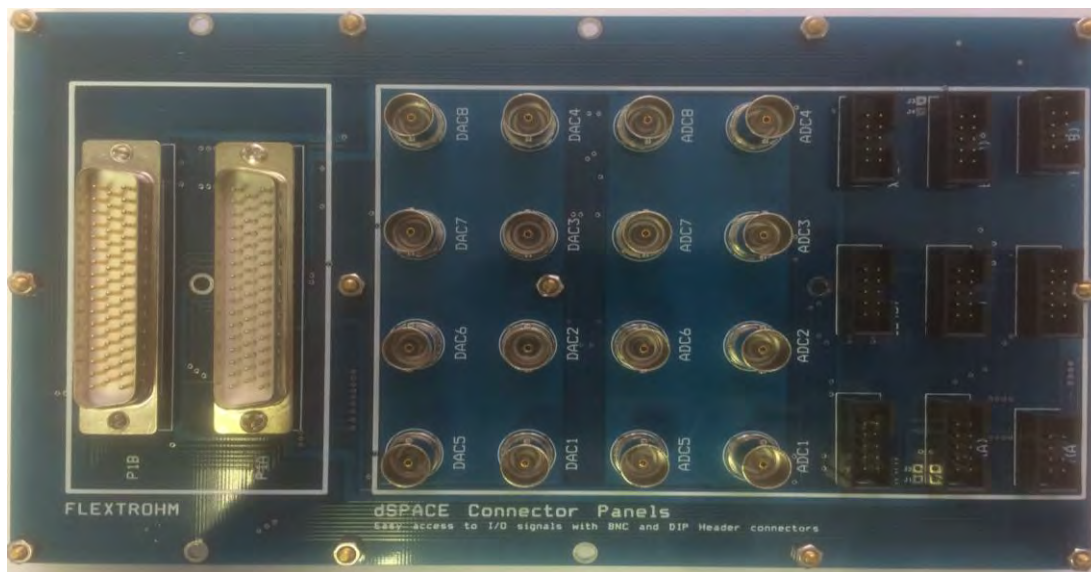


Figure 3.25: Dspace Connector

### 3.9.1 Blanking Time

In theoretical, upper side and lower side switching devices is ideally complementary each other. In practical, both sides of switching devices need to consider the time taken by switching devices to turn-on and turn-off. Short circuit will happen if the both sides of switching devices turn-on simultaneously. In order to avoid the short circuit happened, the blanking time must be programmed in FPGA. FPGA is a microcontroller that been used to compile a program. The blanking time used to make a delay about  $2\mu\text{s}$  for the switching devices turn-on. There are three input signals and twenty four output signals had been program in FPGA based on the construction of proposed switching technique. Figure 3.26 shows the FPGA microcontroller. There are two reasons of using the gate driver when working with control electronic part and power converter. The signals produce from FPGA are insufficient to drive power switches thus, the gate driver is used to amplify the power signals. In addition, gate driver used for safety and proper operation in which twenty-four signals used to drive power switches must be electrically isolated to each other.



Figure 3.26: Microcontroller FPGA

Figure 3.27 represents the block diagram of blanking time generation. The signals will be separated and operate alternately when receive the signals from Dspace.  $S1$  is one of the signals that have been separated while  $\bar{S}1$  represents the contradict signal of  $S1$ . The block Upper Counter will count if the rising edge of the signals is recognised. The comparator block is used to make a delay for the power switches to turn on by comparing with the clock generated.

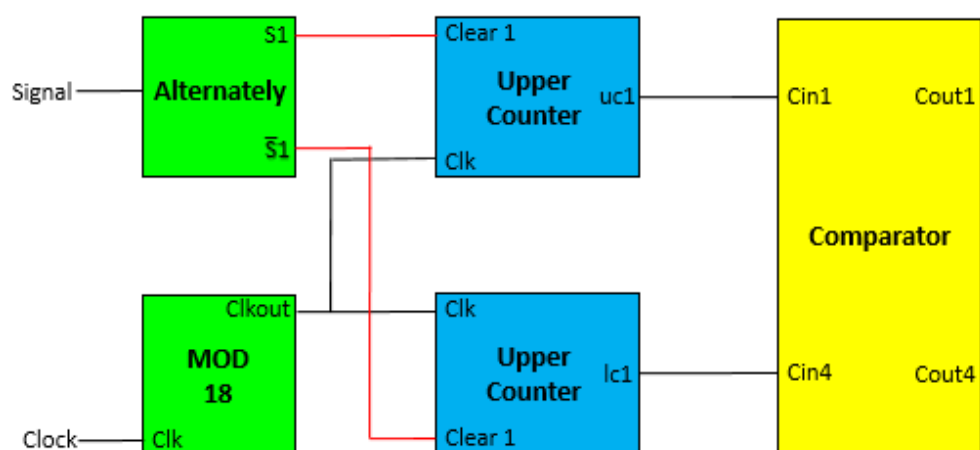


Figure 3.27: Block Diagram of Blanking Time Generation

## 3.10 Flowchart

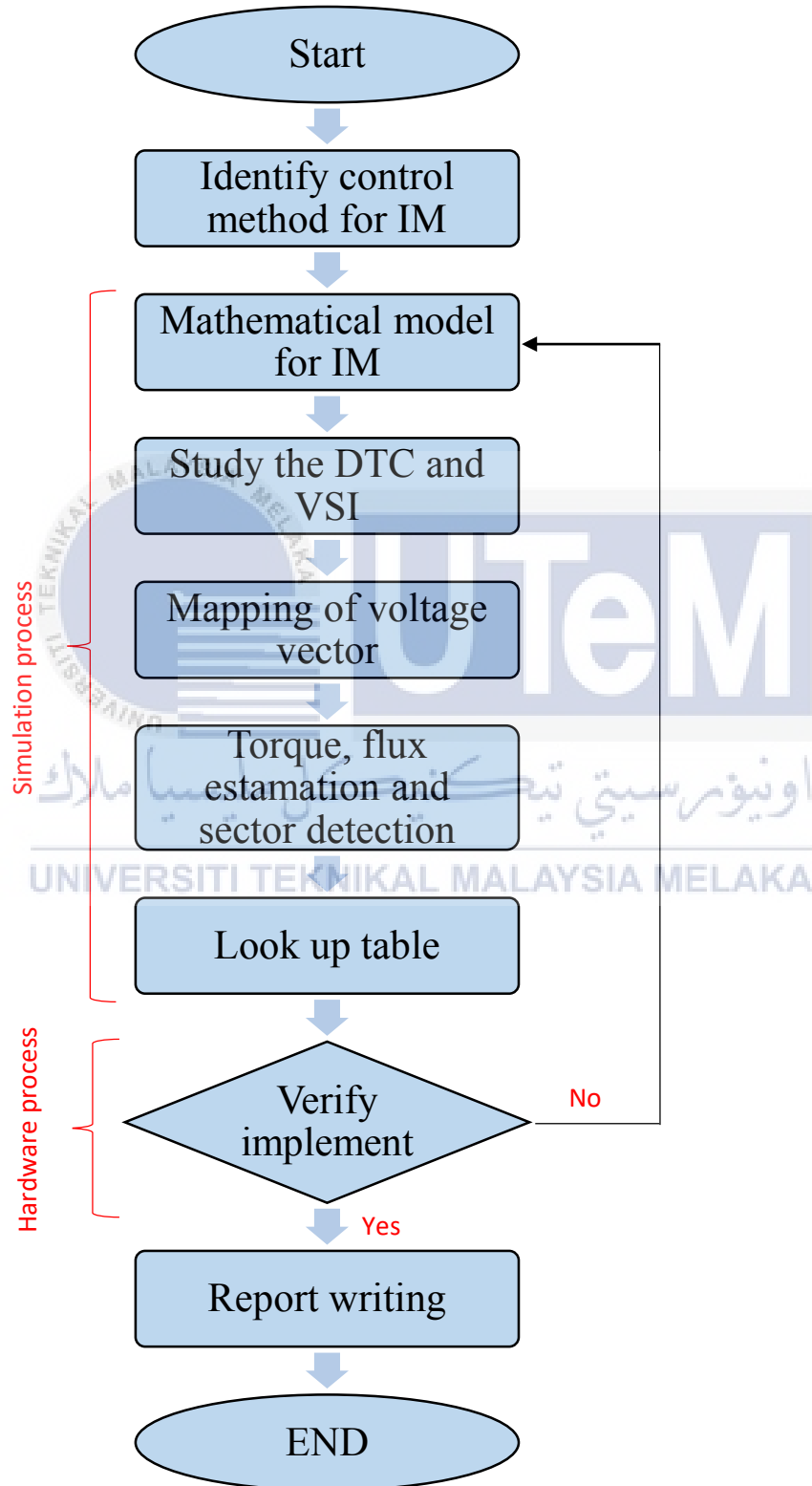


Figure 3.28: Flowchart of Research Methodology

### 3.10 Milestone Research

There are a few milestones set for this project to ensure the project run systematically as planned.

First milestone is to study a concept of induction motor and study the topology circuit of Direct Torque Control (DTC).

Second milestone is to identify the mathematical modelling of induction motor and basic operation of DTC.

Third milestone is to construct the DTC of induction motor in MATLAB software and run the simulation.

Forth milestone is to validate the data obtained from the simulation and compare the results between conventional and proposed.

Fifth milestone for the project is to build up the hardware construction of DTC of induction motor.

Sixth milestone for the project is to verify the proposed technique valid to implement in hardware using FPGA microcontroller.

Seventh milestone for the project is to identify the hardware results and compare with simulation results.

Eighth milestone for the project is writing the report about the findings.

## CHAPTER 4

### RESULT AND DISCUSSION

#### 4.1 Introduction

In this chapter discusses the results obtained from the simulation using MATLAB software. There are two part of result which contains of conventional result and the proposed technique result obtained. There are some explanation and comparison on both results. The results will be analysed on the torque error produced and the switching frequency respectively. In addition, this chapter will discusses the results collected through hardware. Obtained results will be verified by comparing the simulation results and hardware results.

#### 4.2 Conventional Result

Figure 4.1 shows conventional DTC operation circuit designed using MATLAB software. The designed circuit consists of the estimation current of phase a,  $i_a$  and phase b,  $i_b$ . The currents will be compared to identify the sector selection. The torque estimation and flux estimation will be compared with the sector selection to verify in look-up table.

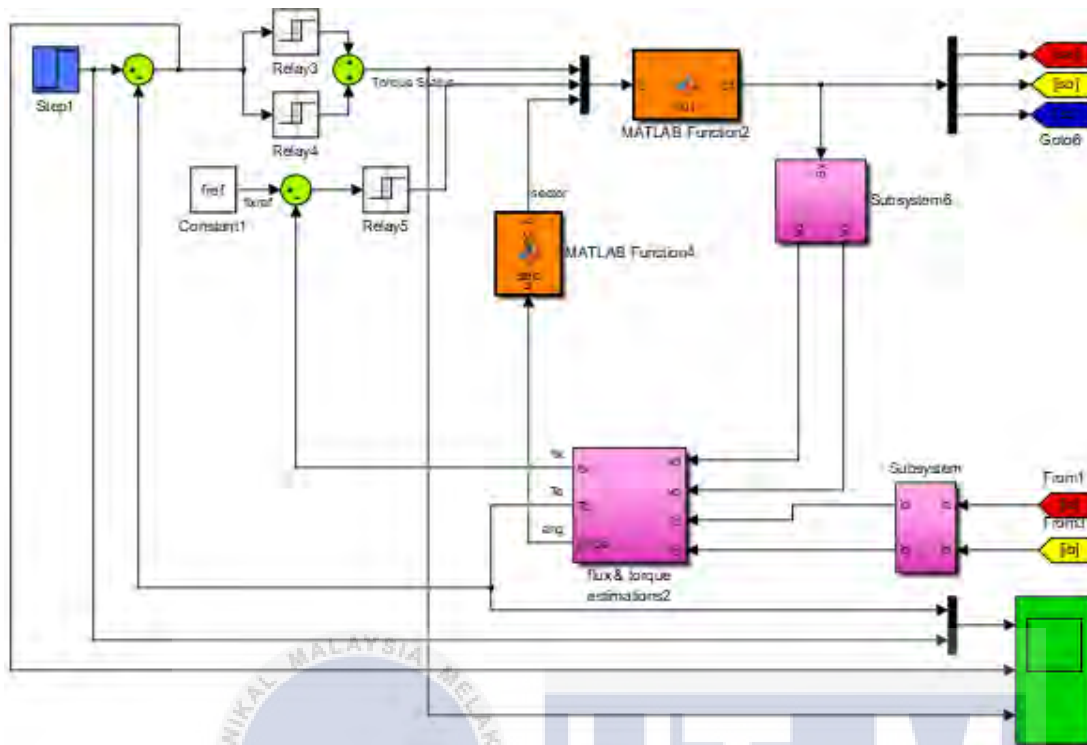


Figure 4.1: DTC Operation Circuit

Figure 4.2 represents the output of torque estimation, torque produced, torque error and torque error status for the conventional DTC of induction motor. Basically, the torque error will be contradict with the torque produced. The torque hysteresis-based controller is being set to  $\pm 0.2$ . When the torque reach  $+0.2$  the torque error status will produced 0 while the torque reach  $-0.2$  the torque error status produced 1. The torque error status will indicate either 1 or 0. The output of torque is being compared with the reference torque as shown in figure below. Figure 4.3 shows the comparison between estimation of torque, torque produced, torque error and torque error status.

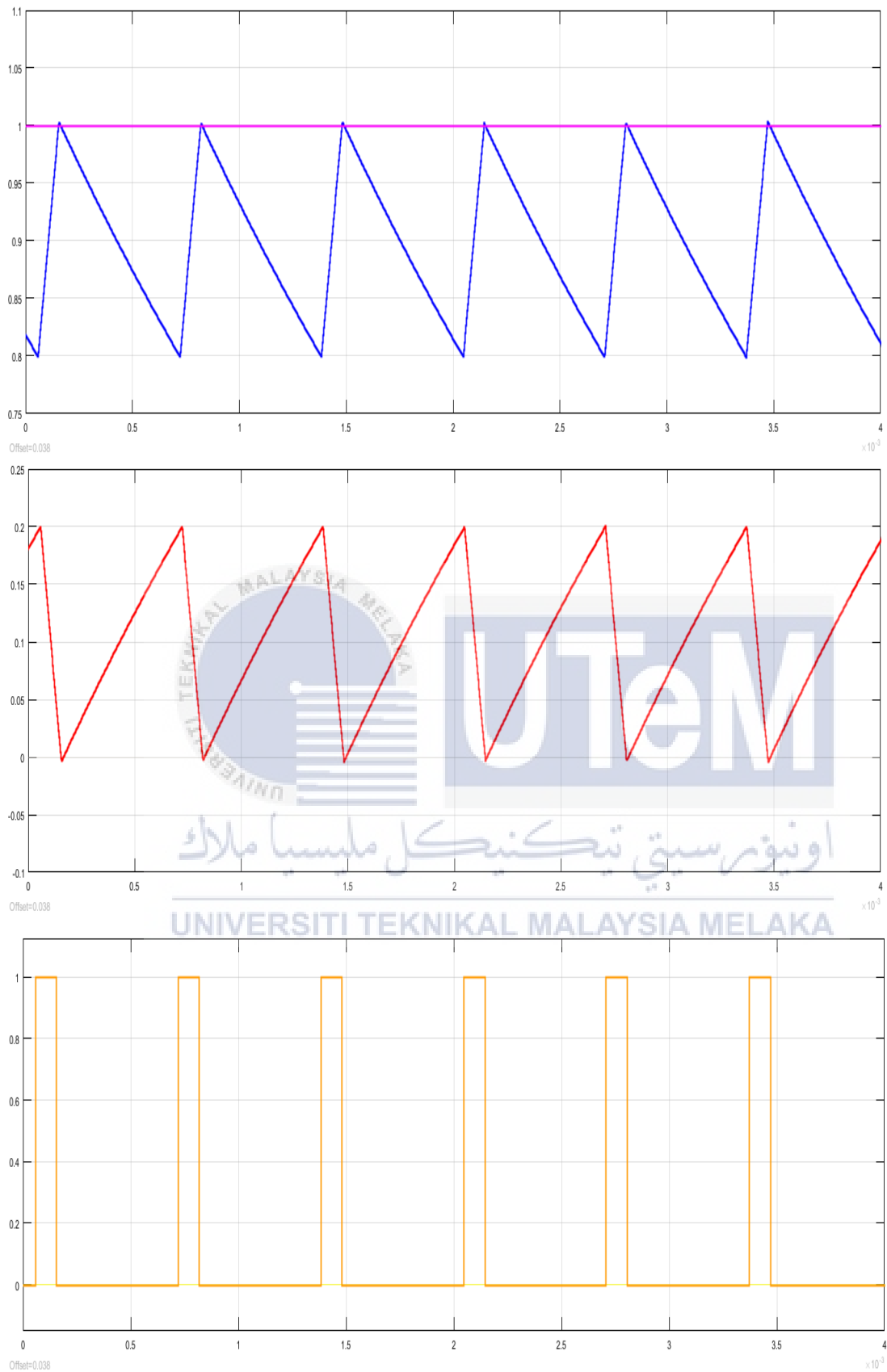


Figure 4.2: Estimation Torque, Torque, Torque Error & Torque Error Status

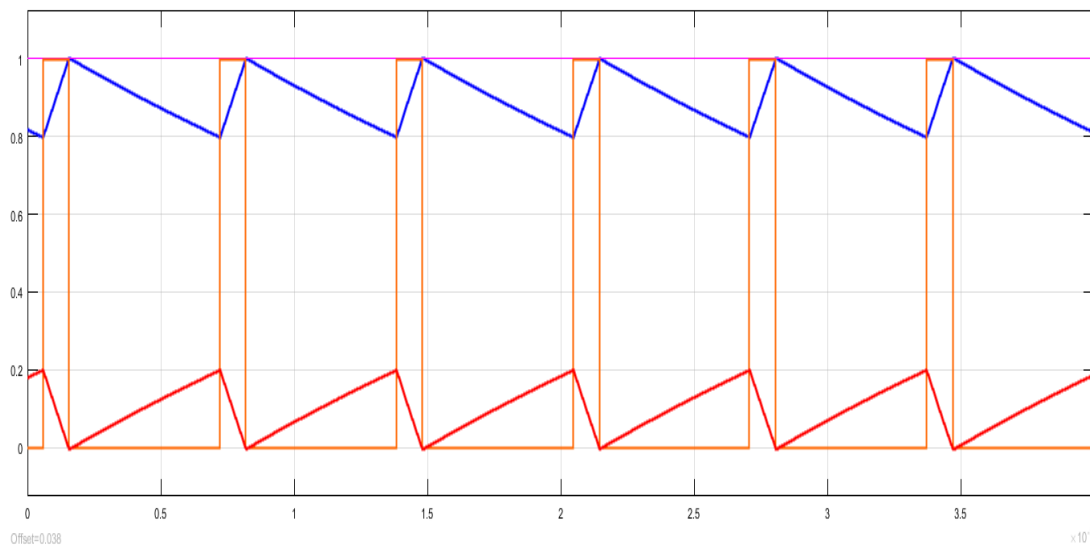


Figure 4.3: Comparison of Waveforms

The switching frequency obtained as the operation of the DTC conducted. The Voltage Source Inverter (VSI) consists of three legs. Every legs consist of two switching devices as shown in Figure 4.4. The two switching devices for each legs must be complementary for each other. Both switching devices for each legs have to operate contradictory to ensure there is no short circuit happened. Figure 4.5 shows the connection of VSI and fed into the induction motor.

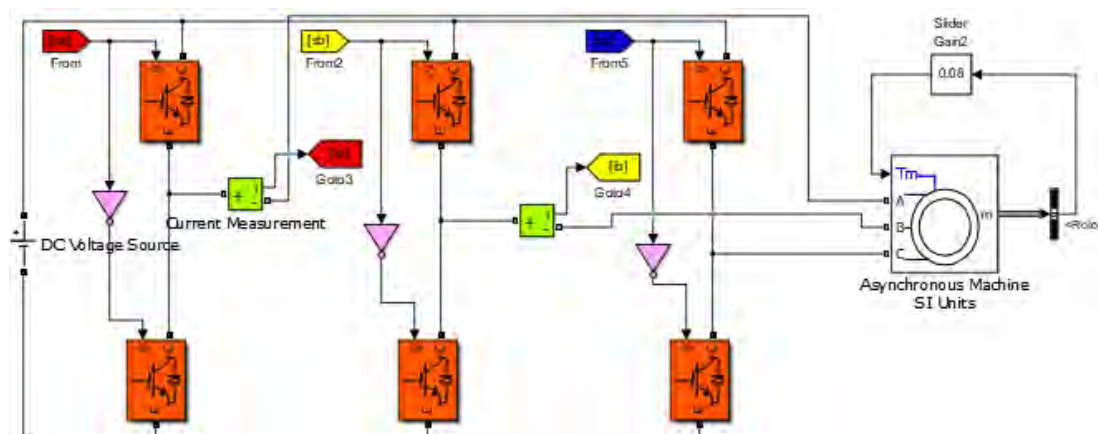


Figure 4.4: VSI Connection

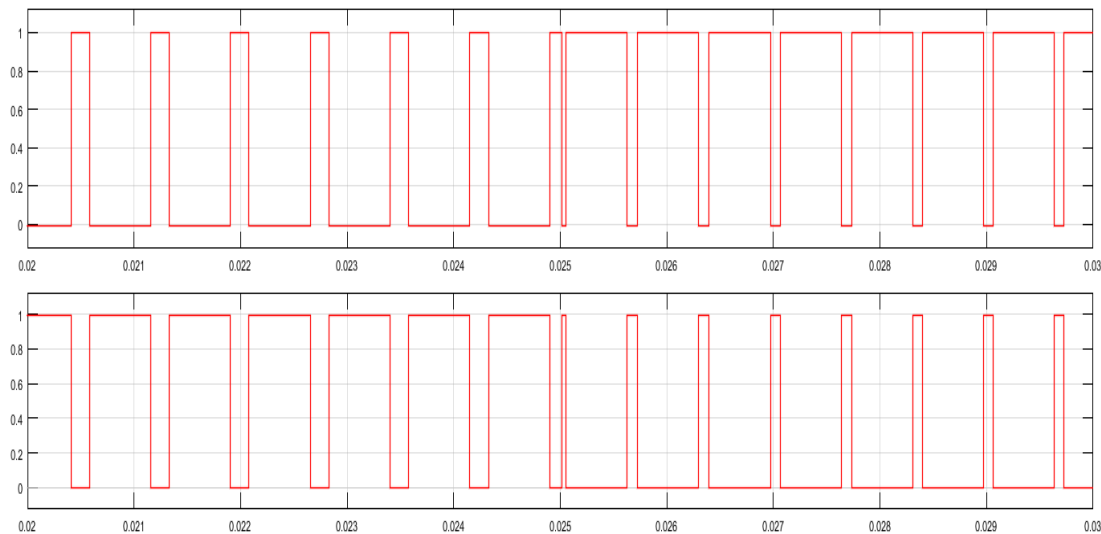


Figure 4.5: Switching Frequency of VSI

### 4.3 Proposed Technique Simulation Result

As mentioned above, the purpose of proposed technique is to improve the performance of Direct Torque Control (DTC) of induction motor. Figure 4.6 shows the configuration of the DTC. The same figure as the conventional of DTC configuration is used. The different is the band of hysteresis-based torque controller. The band is being minimize to produce a torque closed to the reference torque. So, there will be less torque error produced. In addition, minimizing the band will increase the switching frequency.

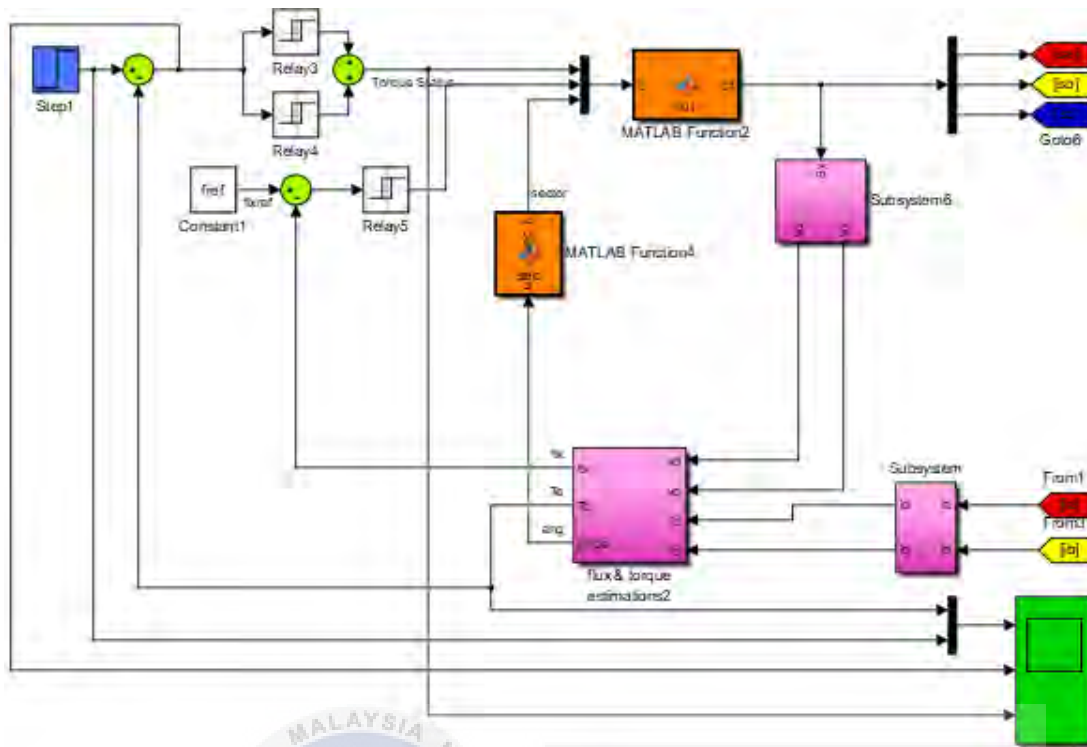


Figure 4.6: Configuration of DTC

Figure 4.7 represents the output of torque estimation, torque produced, torque error and torque error status for the conventional DTC of induction motor. Basically, the torque error will be contradict with the torque produced. The torque hysteresis-based controller is being set to  $\pm 0.1$ . When the torque reach  $+0.1$  the torque error status will produced 0 while the torque reach  $-0.1$  the torque error status produced 1. The torque error status will indicate either 1 or 0. The output of torque is being compared with the reference torque as shown in figure below. Figure 4.8 shows the comparison between estimation of torque, torque produced, torque error and torque error status.

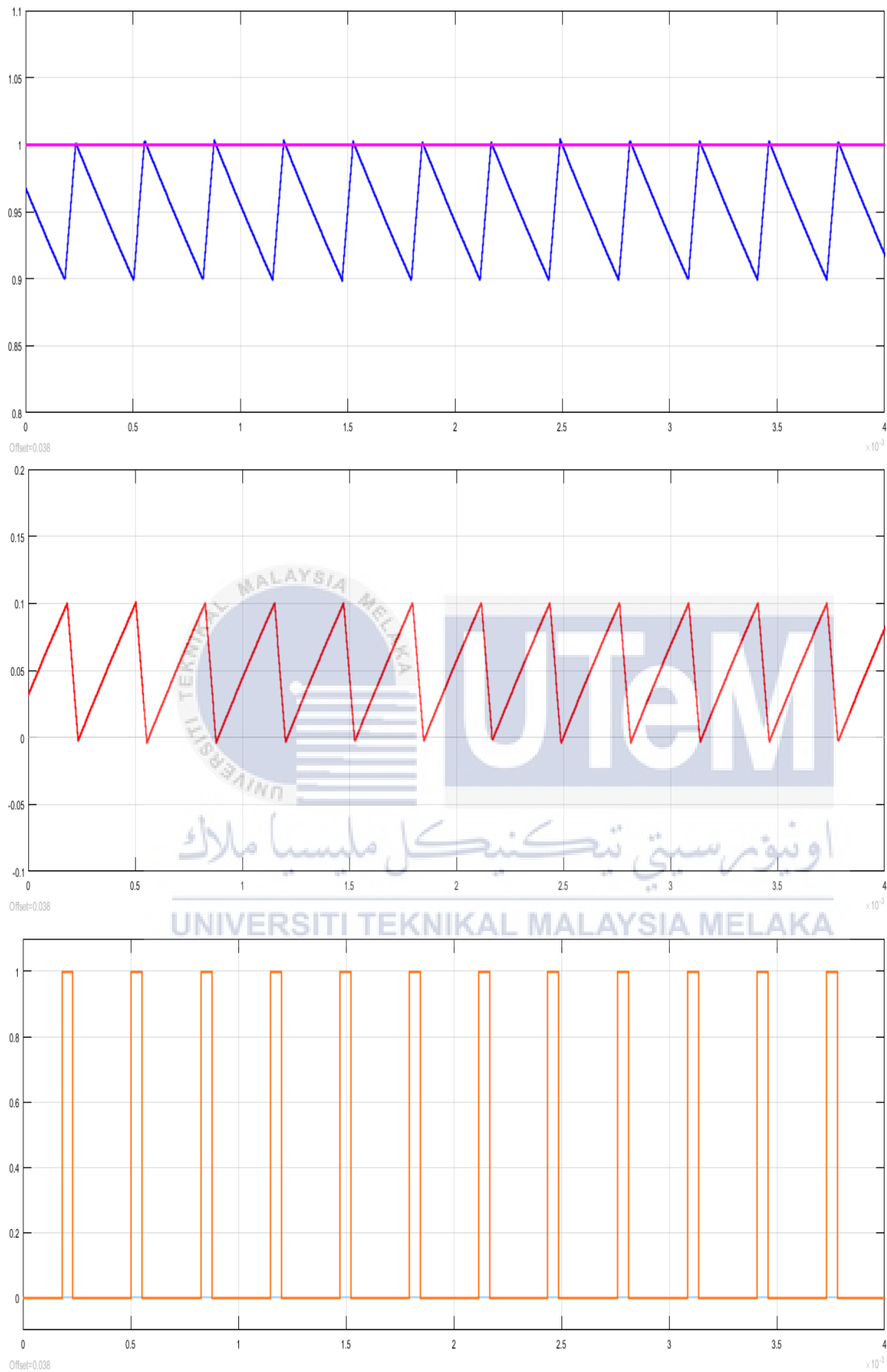


Figure 4.7: Reference Torque, Torque, Torque Error & Torque Error Status

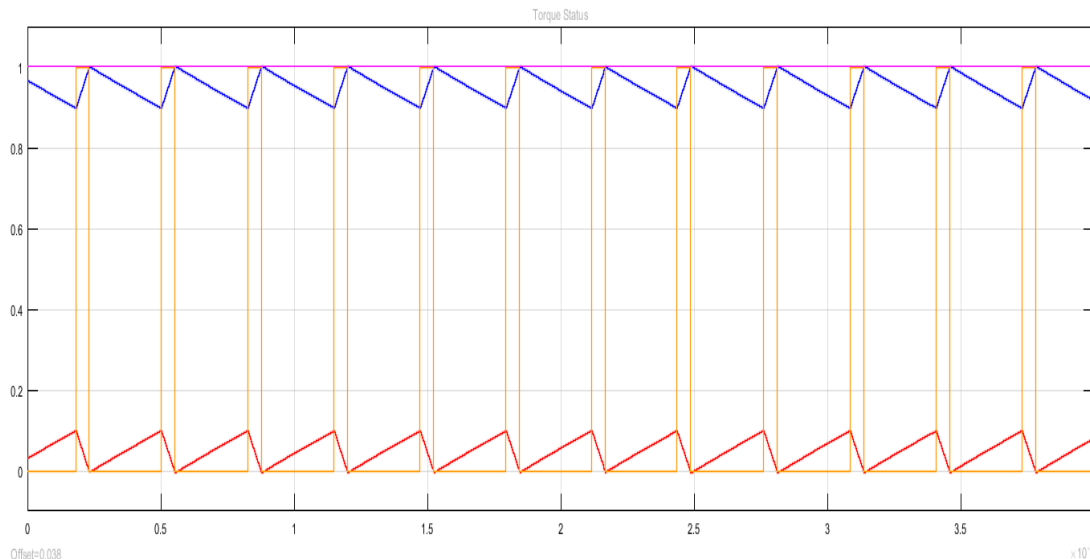


Figure 4.8: Comparison of Waveforms

Figure 4.9 represent 1<sup>st</sup> leg of Voltage Source Inverter (VSI). The simulation results is used to be compared with the conventional results. The results prove if the band of hysteresis-based torque controller has been reduced, the switching frequency will become more frequent. If the often frequency is being implemented to hardware, it will degrade the switching devices performance. The rapidly switching frequency also will produce heat at the switching devices. The heat will cause thermal losses due to present of high voltage drop at the switching device. Figure 4.10 shows the proposed technique for the switching devices to ensure the switching devices operate at optimal performance. The proposed switching devices are connected in parallel with a group of four switching devices as shown in figure below. For every subsystem will be connected to the proposed switching devices in VSI. Theoretically, by connecting the devices in parallel will produce same voltage drop through each of the devices. In this experiment, the switching devices will operate at different time with different input signal. So, the switching devices do not have to operate rapidly and frequently.

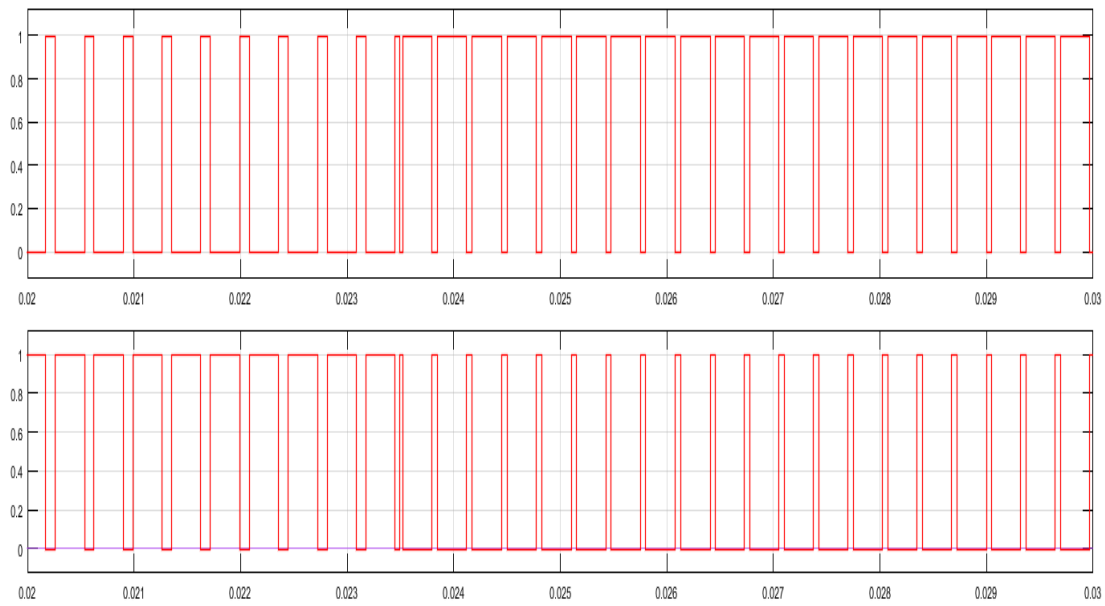


Figure 4.9: 1<sup>st</sup> Leg Switching Frequency of VSI

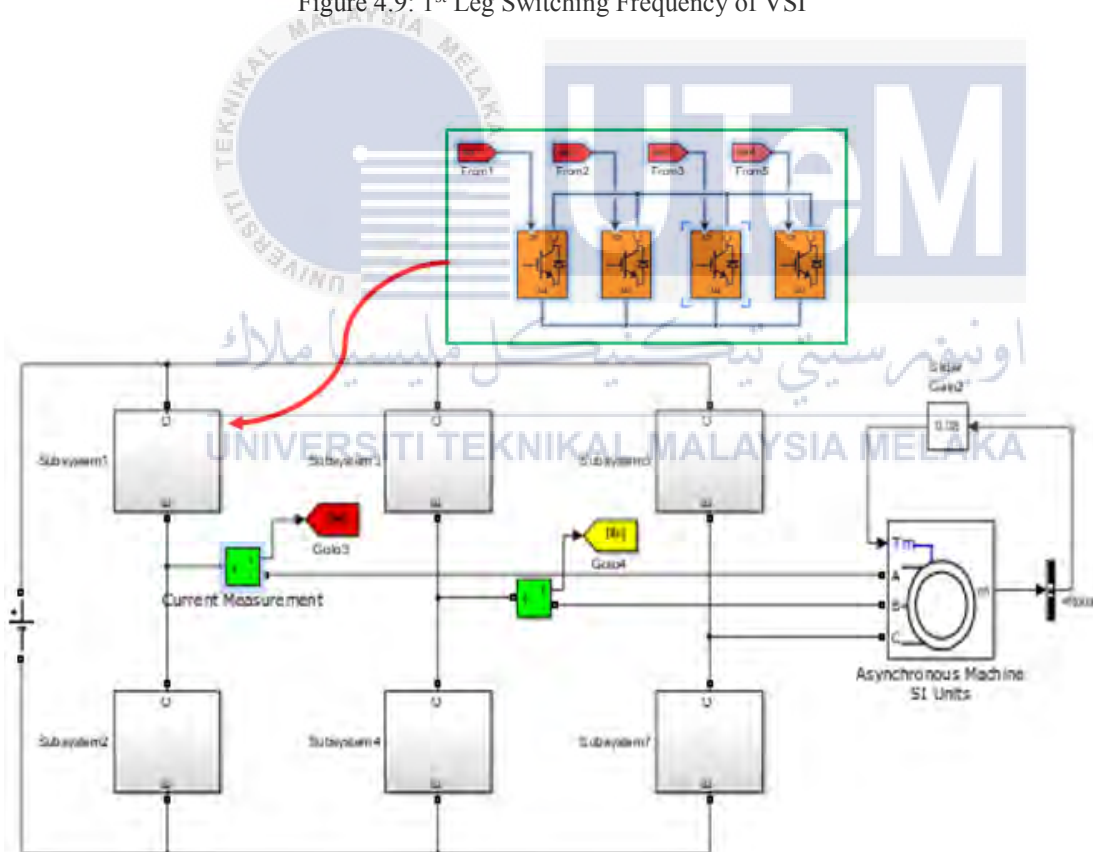


Figure 4.10: Proposed Strategy

In theoretical, the Voltage Source Inverter (VSI) consist of three legs and each legs provided two switching devices. The proposed switching technique, VSI also consists of three legs but each legs have eight switching devices, four IGBTs for upper side and four IGBTs for lower side. Figure 4.11 represent the upper signal that will be injected to the 1<sup>st</sup> leg in Voltage Sources Inverter (VSI). The upper signal will be inverted to produce signal for lower side of the 1<sup>st</sup> leg. The signal will be divided into four signals and will be supplied to each of the Integrated Gate Bipolar Transistors (IGBTs) for upper side of the 1<sup>st</sup> leg VSI. Figure 4.12 shows the IGBTs operate alternately follow the sequence of the signal.

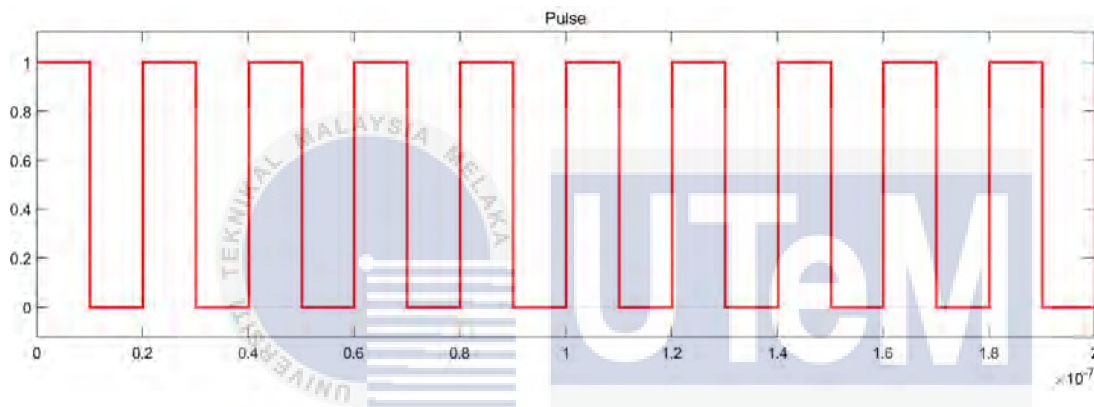


Figure 4.11: Pulses

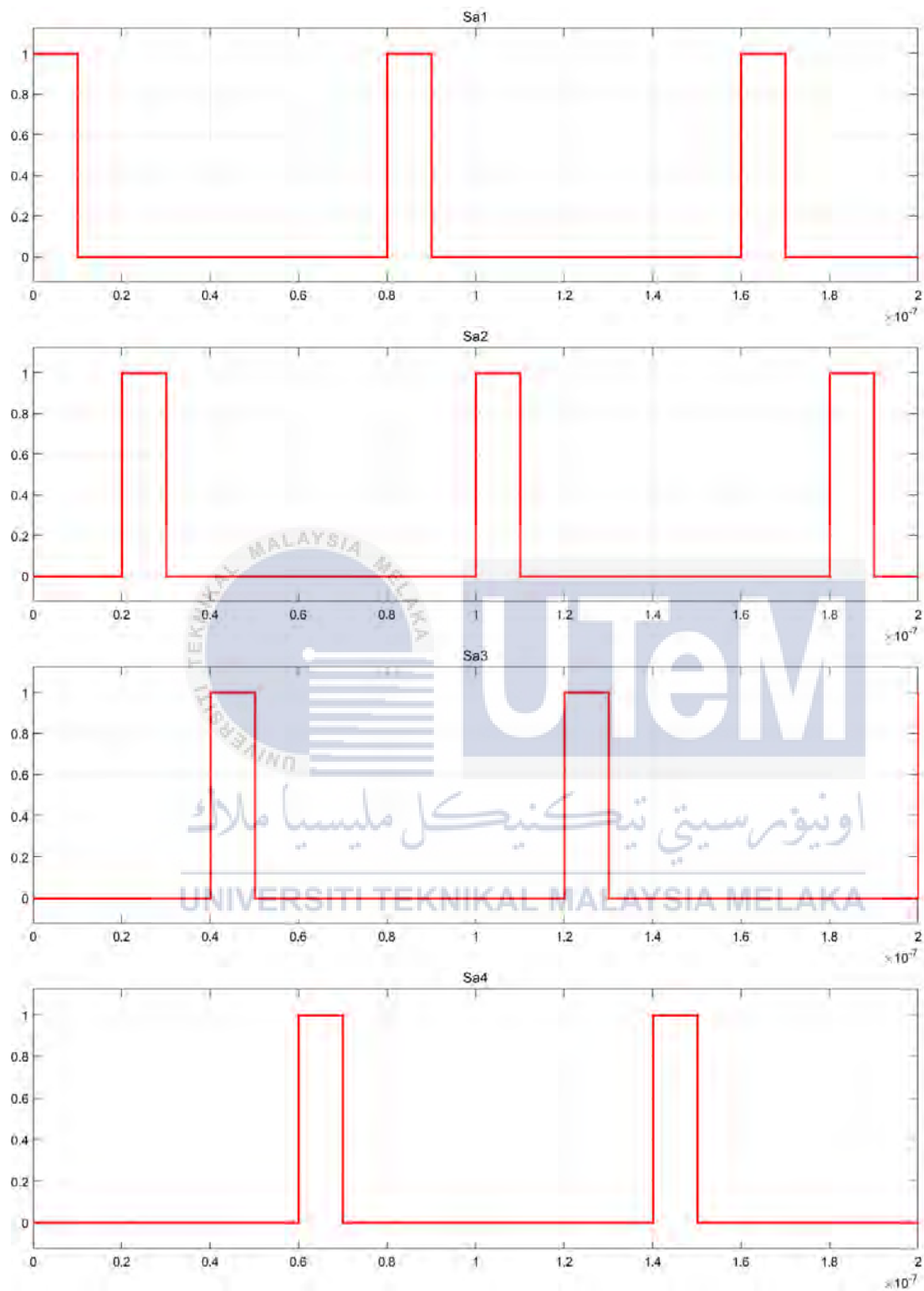


Figure 4.12: Switching Devices Operate Alternately

Figure 4.13 represents the phases current produced by phase  $a$  and phase  $b$ . Both phases must be shifted  $90^\circ$ . The structure of Direct Torque Control (DTC) of induction motor shows the both phases current must be calculated to produce the vector current  $i-d$  and  $i-q$ . Both vector currents produced will send information to look-up table to make comparison between torque and flux produced.

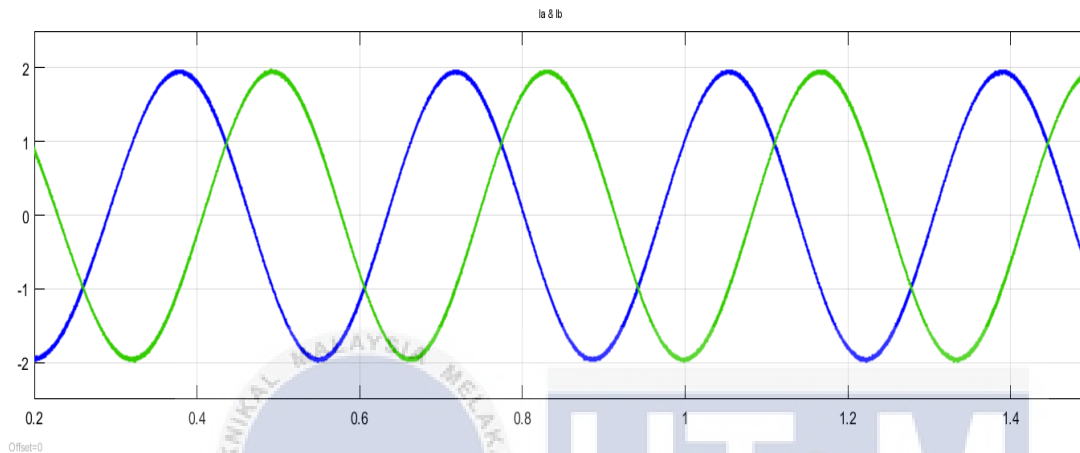


Figure 4.13: Phases Current

#### 4.4 Hardware Result

Figure 4.14 shows the results obtained for the upper side of 1<sup>st</sup> leg of Voltage Source Inverter (VSI). One of the objectives have been achieved because the switching devices are operating alternately as proposed technique. The implementation of blanking time in microcontroller FPGA prevents the VSI become short circuit. The program in the microcontroller provides the instructions for the switching devices operate alternately. Figure below proved the alternates operation of switching devices. The black signal represented the input signal that will be fed in VSI. The coloured signal represented each of the switching devices respectively. Figure 4.15 represent the lower side of switching devices. The black signal in Figure 4.15 represents the upper side input signal to prove the signal is contradictory and being separated into four signals.

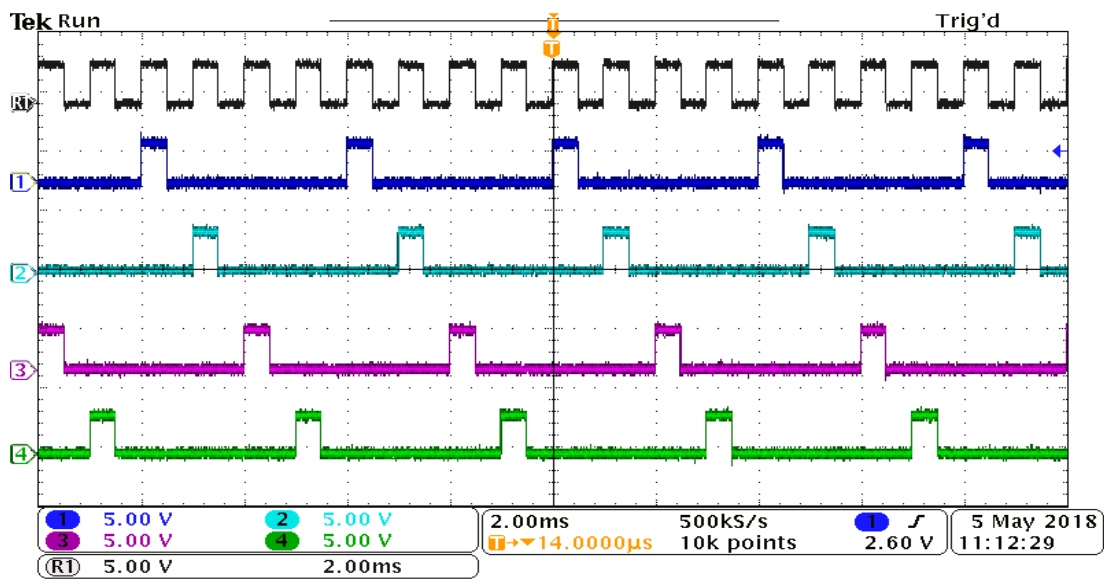


Figure 4.14: Proposed Switching Technique

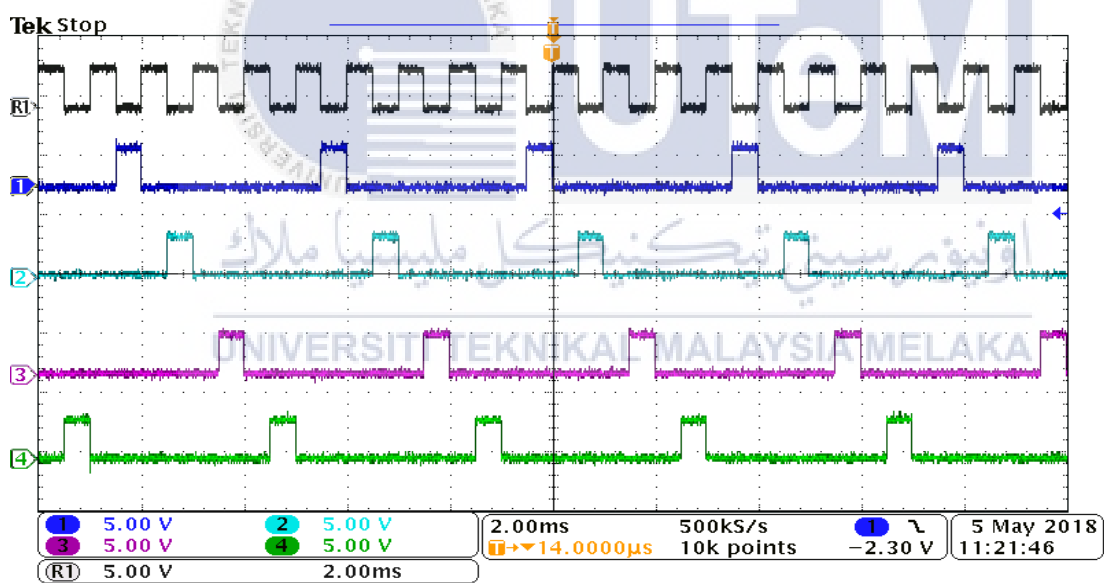


Figure 4.15: Proposed Switching Technique

Figure 4.16 proves the dead time for the signals of the gate driver. The signals take about  $2\mu\text{s}$  delay to turn on. The purpose of the delay is to prevent the signals for upper side and lower side to turn on simultaneously. The power converter circuit could become short circuit and the induction motor can be drives.

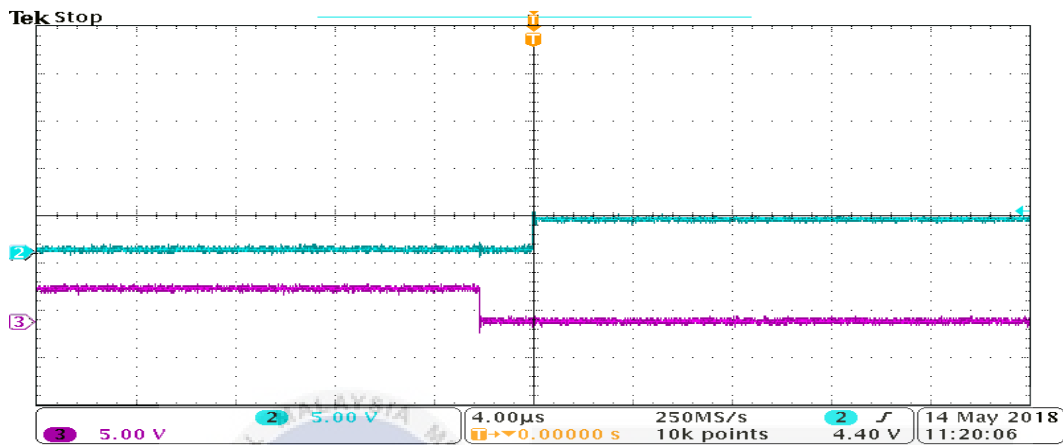


Figure 4.16: Dead Time

Figure 4.16 shows the results of phases current *a* and *b*. The phases currents do not produced as well as the simulation results. It is might be caused by the noises or disturbances of surrounding. Ideally, the phases current must be sinusoidal to drives the motor smoothly. The motor is being drives by the power converter. The power converter is injected by 50V power supply.

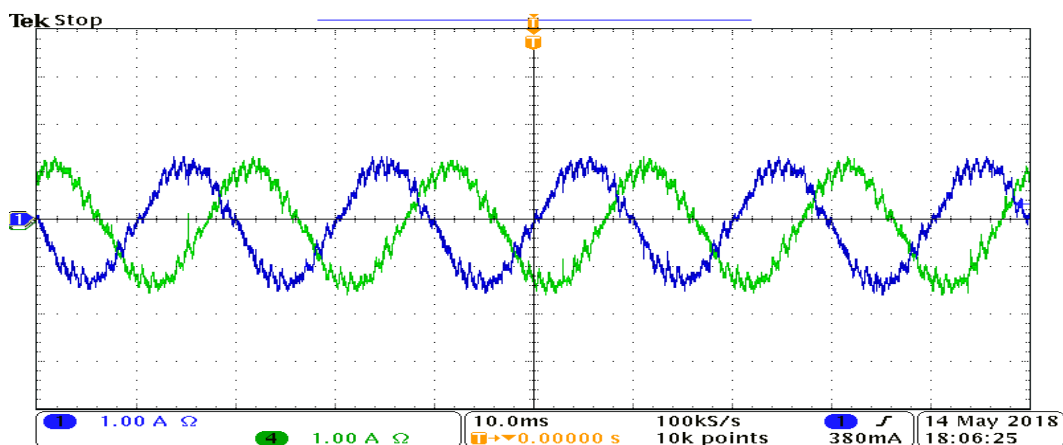


Figure 4.17: Phases Current

## CHAPTER 5

### CONCLUSION AND RECOMMENDATION

#### 5.1 Conclusion

This thesis has presented improvements of Direct Torque Control (DTC) of induction motors, in terms of reducing the torque by using hysteresis based controller and proposed optimal switching strategy using Voltage Source Inverter (VSI). Most of previous works do not solve the problems simultaneously. Several works attempt to reduce the torque ripple. In fact, reducing the torque ripple will enlarge the switching frequency. This problem will cause degradable of the switching devices as there are thermal losses occur. Higher switching frequency also can cause reduction of the switching devices performance. The major effect of torque is the current flow. If the torque increases, the current will also increase. The main reduction of torque is to prevent current losses. There are many papers attempt by reducing the torque but neglecting the other factors that affect the performance of induction motor. This thesis improves the performance of induction motor by reducing the torque by decreasing the tolerant band of hysteresis controller and proposed a new strategy of switching technique as to ensure the switching devices operate at optimal performance and prevent the degrade of the switching devices. Finally, the main benefit of this proposed techniques is two improvements can be achieved simultaneously.

## 5.2 Recommendation

For the future works, the improvement of Direct Torque Control (DTC) of induction motor should be consider the optimal switching technique and reduces the implementation cost. The switching technique is the main part to control the switching frequency. The main purpose for the optimal switching technique is for prevention of degradable switching devices. Previous researchers are aiming for reducing the torque. However, torque decreasing will cause switching frequency increase. Thus, optimal switching technique must be used to protect the switching devices. In addition, the cost for hardware implementation should be consider to prevent wastage.



## REFERENCES

- [1] M. Khairi Rahim, Auzani Jidin, Tole Sutikno. "Enhanced Torque Control and Reduced Switching Frequency in Direct Torque Control Utilizing Optimal Switching Strategy for Dual Inverter Supplied Drive", International Journal of Power Electronics and Drive Systems, 2016
- [2] Zou, Gan, Tao Li, and Ren Xin Xiao. "Induction Motor Direct Torque Control Based on Multiple Neural Networks Optimized by Genetic Algorithm", Advanced Material Research, 2012.
- [3] Mohanty, Kanungo Barada. "A Direct Torque Controlled Induction Motor with Variable Hysteresis Band", 11<sup>th</sup> International Conference on Computer Modelling and Simulation, 2009
- [4] A.S. Carvalho. "Technological trends in induction motor electrical drives", IEEE Porto Power Tech Proceedings, 2001
- [5] Jezernik, K., J. Korelic, and R. Horvat. "PMSM sliding mode FPGA-based Control for Torque Ripple Reduction", IEEE Transactions on Power Electronics, 2012.
- [6] Ronak V. Nemade, Jay K. Pandit, Mohan V. Aware. "Reconfiguration of T-Type Inverter for Direct Torque Controlled Induction Motor Drives Under Open-Switch Faults", IEEE Transactions on Industry Applications, 2017
- [7] Cheng Shao. "Novel Hybrid Sliding-mode Controller for Direct Torque Control Induction Motor Drives", 2006 American Control Conference, 2006
- [8] Yaohua Li. "The control of stator flux and torque in the surface permanent magnet synchronous motor direct torque control system", 2009 4th IEEE Conference on Industrial Electronics and Applications, 2009
- [9] Sarode, Dipali, Arti Wadhekar, and Rajesh Autee. "Voltage source inverter with three phase preventer and selector for industrial application", International Conference 2015
- [10] A. F. Sakr. "Particle Swarm Optimized Direct Torque Control of Induction Motors", IECON 2006 - 32nd Annual Conference on IEEE Industrial Electronics, 2006
- [11] Yusnida Tarmizi, Auzani Jidin, Kasrul Karim, S. Azura Tarusan, M. Khairi Rahim, R. Sundram, Huzainirah Ismail. "Investigation of torque and flux-current producing components in indirect rotor flux oriented control (IRFOC) of induction machines", 2015 IEEE Student Conference on Research and Development (SCOReD), 2015

- [12] Eremia, Mircea, and Constantin Bulac. "Synchronous Generator and Induction Motor", Handbook of Electrical Power System Dynamics Modeling Stability and Control, 2013.
- [13] Krishnaveni, D., A. Sivaprakasam, and T. Manigandan. "Optimum voltage vector selection in Direct Torque Controlled PMSM using intelligent controller", 2014 International Conference on Green Computing Communication and Electrical Engineering (ICGCCEE), 2014
- [14] K. L. Shi, T. F. Chan, Y. K. Wong, S.. "A New Acceleration Control Scheme for an InverterFed Induction Motor", Electric Machines & Power Systems, 4/1/1999
- [15] Gao, Sheng-wei, and Yan Cai. "Torque Ripple Minimization Strategy for Direct Torque Control of Induction Motors", 2010 Third International Conference on Intelligent Networks and Intelligent Systems, 2010.
- [16] Yahya Ahmed Alamri, Nik Rumzi Nik Idris, Ibrahim Mohd. Alsofyani, Tole Sutikno. "Improved Stator Flux Estimation for Direct Torque Control of Induction Motor Drives", International Journal of Power Electronics and Drive Systems (IJPEDS), 2016
- [17] Jidin, Auzani, Nik Rumzi Nik Idris, Abdul Halim Mohamed Yatim, Tole Sutikno, and Malik E. Elbuluk. "Simple Dynamic Overmodulation Strategy for Fast Torque Control in DTC of Induction Machines With Constant-SwitchingFrequency Controller", IEEE Transactions on Industry Applications, 2011.
- [18] Prasad, D.. "Digital simulation and hardware implementation of a simple scheme for direct torque control of induction motor", Energy Conversion and Management, 2008.

## APPENDIX A

```

%Induction machine parameters
Rs = 6.1;
Rr = 6.2298;
Ls = 0.47979; %Stator self inductance
Lr = 0.47979; %Rotor self inductance
Lm = 0.4634; %Mutual inductance
P = 1; %number of poles
J = 0.01; % moment of inertia
B = 0; %viscous friction

Lls=Ls-Lm;      %Stator leakage inductance
Llr=Lr-Lm;      %Rotor leakage inductance

%Control system parameters
HBT = 0.2; %torque hysteresis bandwidth
HBF = 0.8452*0.001; %Torque hysteresis bandwidth
fref = 0.8452; % reference flux = 0.8452
DT = 1e-6; %sampling period
Vdc = 240; %DC voltage

```



## APPENDIX B

```
function sec_k = sec(u)

%* u[1] = angle, y[0] = sector */

sector=0;
angle = u(1);

if( (angle >= -pi/6) && (angle < pi/6))
    sector = 2;
elseif ((angle >= pi/6) && (angle < pi/2))
    sector = 3;
elseif ((angle >= pi/2) && (angle < 5*pi/6))
    sector = 4;
elseif ((angle >= 5*pi/6) || (angle < -5*pi/6))
    sector = 5;
elseif ((angle >= -5*pi/6) && (angle < -pi/2))
    sector = 6;
elseif ((angle >= -pi/2) && (angle < -pi/6))
    sector = 1;
end

sec_k =[sector];
end
```

اوتیور سیتی تکنیکل ملیسیا ملاک

UNIVERSITI TEKNIKAL MALAYSIA MELAKA

